Thesis for a Ph. D. Degree

Characteristic large-scale circulation pattern of the persistent droughts of Northeast Asia from premonsoon season to monsoon season

몬순 전부터 몬순기간까지
북동아시아지역 지속성 가뭄의 대기 순환장 특성

2014

School of Earth and Environmental Sciences
Graduate School
Seoul National University

Jong-Seo Park

Characteristic large-scale circulation pattern of the persistent droughts of Northeast Asia from premonsoon season to monsoon season

By
Jong-Seo Park

A Dissertation submitted to the Faculty of the Graduate School of the Seoul National University in partial fulfillment of the requirements for the Degree of Doctor of Philosophy

Degree Awarded:
February 2014

Advisory Committee:

Professor In-Sik Kang, Chair
Professor Gyu-Ho Lim, Advisor
Professor Jong-Ghap Jhun
Professor Dong-Kyou Lee
Professor Sang-Wook Yeh

이학박사학위논문

몬순 전부터 몬순기간까지
북동아시아지역 지속성 가뭄의 대기 순환장 특성

Characteristic large-scale circulation pattern of the persistent droughts of Northeast Asia from premonsoon season to monsoon season

2014년 2월

서울대학교 대학원
지구환경과학부
박 종 서

Characteristic large-scale circulation pattern of the persistent droughts of Northeast Asia from premonsoon season to monsoon season

몬순 전부터 몬순기간까지 북동아시아지역 지속성 가뭄의 대기 순환장 특성

지도교수 임 규 호

이 논문을 이학박사 학위논문으로 제출함
2013년 10월

서울대학교 대학원
지구환경과학부
박 종 서

박종서의 이학박사 학위논문을 인준함
2013년 12월

위 원 장 _____(인)

부위원장 _____(인)

위 원 _____(인)

위 원 _____(인)

위 원 _____(인)

Abstract

Characteristic patterns of atmospheric circulation anomalies over the northeast Asian region in the dry and wet premonsoon seasons have been analyzed. The relationship between these patterns in the premonsoon season and the precipitation anomalies in the monsoon season has been also investigated. Since this study focuses on dry premonsoon season, features of anomalous large-scale atmospheric circulations during springtime droughts that occurred over the northeast Asia are revealed. The Palmer drought severity index is used in order to define drought years. In drought years, the anomalous circulation over the northeast Asia exhibits the weakened northward flow from the western North Pacific, and the position of the East Asian westerly Jet (EAWJ) maximum core at 300hPa is shifted southward. Thus, the rainfall band is moved southward, and the associated precipitation is suppressed over Korea, Japan, and southeastern China during spring droughts. The Sea Surface Temperature (SST) anomalies and outgoing longwave radiation anomalies, which show a north–south dipole pattern between the Philippines and the northeast Asian region, support these dry conditions through the Hadley circulation. The anomalously warm SSTs in the western North Pacific seem to play an important role in the atmospheric circulation associated with persistent northeast Asian droughts

The persistent features of extreme precipitation over the northeast Asia from

premonsoon season to monsoon season are found. In order to understand some characteristics of the circulation anomalies associated with persistent features of extreme precipitation, six dry cases and six wet cases in the premonsoon season are selected. Both of the extreme conditions are nearly persistent in each case. As mentioned in spring drought analysis, the weakened western North Pacific subtropical high (WNPSH) and the southward-shifted EAWJ are predominant for dry cases. For wet cases, the strengthening of WNPSH, the northward-shifted EAWJ in spring, and southward-shifted EAWJ in summer are apparent. However, dry cases are associated with the warm SST anomalies of the western North pacific, whereas wet cases are related to the warm SST anomalies of the Indian Ocean and Bay of Bengal. The dependency of extreme precipitation on this SST anomaly pattern is supported through numerical experiments. Based on the observational analysis and model experiments, the main connection system between extreme precipitation such as drought and SST is the anomalous cyclonic circulation over the western North Pacific.

Key words : western North Pacific subtropical high, drought, East Asian Westerly Jet Index, premonsoon, persistent feature

Table of Contents

List of Figures

List of Table

1. Introduction

The East Asian summer monsoon (EASM) is characterized by (1) a low-level convergence zone between southerlies from the tropics and northerlies from the mid-latitude regions and (2) an upper tropospheric westerly to the north of the western North Pacific subtropical high (WNPSH) (Wang and Xu, 1997; Wang et al., 2004; Gong and Ho, 2003). The north-south displacement of the East Asian westerly jet (EAWJ) plays a key role in determining the onset and retreat of the summer monsoon rainfall band in East Asia (Liang and Wang, 1998). The strong year-to-year variation of the summer monsoon is usually responsible for severe floodings or droughts over East Asia. Severe droughts are often connected with stagnated large-scale circulation systems and occur when there is an abnormal evolution of the seasonal cycle, such as when there is an early development of the upper level anticyclonic flow over East Asia (Park and Schubert, 1997).

The premonsoon season is a relatively dry period prior to the onset of the Asian summer monsoon (Wang and Xu, 1997). There is a climatological dry singularity from mid-May to mid-June before Changma in Korea (Byun, 1991). Spring rainfall of premonsoon season in northeast Asia is usually light but is

nonetheless crucial for the success of crops. Severe spring droughts can lead to agricultural disasters and result in social and economic losses. Drought has been recognized as a reversal feature of severe rainfall and many studies actually focus on monsoon rainfall anomalies. Therefore, the characteristic features and mechanisms of droughts have not been well documented thus far. Moreover, most previous studies have concentrated on specific droughts over local regions.

In a case study of a 1994 summer drought over East Asia, Park and Schubert (1997) suggested that the East Asia summer drought in 1994 was closely associated with the early development of upper-level anticyclones rather than with tropical Pacific sea surface temperature (SST) anomalies. The anomalous circulation suppresses the moisture supply from the Indian Ocean and southern flank of the Western North Pacific subtropical high (WNPSH). Meanwhile, Guan and Yamagata (2003) recently suggested that the east–west dipole pattern of the SST in the Indian Ocean was one of the major causes of the 1994 summer drought.

Indeed, droughts are not generated by a single cause but by multiple causes (Palmer and Brankovic, 1989; Mo *et al*., 1991; Namias, 1991). In order to understand the phenomena and associated physical processes, droughts must be examined in relation to teleconnection and atmospheric circulation anomalies (Namias, 1982). Previous studies have shown that the north–south displacement

of the East Asian westerly jet (EAWJ) (Liang and Wang, 1998) and the intense variation in the WNPSH (Wu and Wang, 2000) are related to summer rainfall anomalies over East Asia. Strong convection in the Western Pacific, especially over the Philippine Sea, is associated with the EAWJ and the WNPSH (Lu, 2004).

The EASM varies year to year, with the onset of the summer monsoon sometimes delayed owing to the dry singularity of the premonsoon period (Wang and Wu, 1997). This abnormal seasonal cycle results in little summer monsoon rainfall (Park and Schubert, 1997). These previous studies imply that the atmospheric circulation conditions of the premonsoon season may influence the onset of the summer monsoon and its associated rainfall variation.

Although large-scale circulation variations in the pre-monsoon season can play an important role in determining when the summer monsoon begins and what affects the rainfall variations, the effect of anomalous circulation in the premonsoon season (spring) is not well documented. Therefore, the purpose of this study is to demonstrate the large-scale circulation variability that occurs in the premonsoon season and to investigate the relationship between anomalous circulations in the premonsoon and summer monsoon periods in East Asia. In addition, this study provides possible mechanisms that may lead to dry and wet conditions.

This work is carried out through both observational analyses and numerical experiments. Section 2 explains the data set and methods used in the study. In section 3 prominent features of large-scale atmospheric circulation during spring drought are described, and section 4 deals with characteristics of anomalous circulation in the spring and the following summer. In section 5, the results of model experiments are shown, and section 6 discuss summaries and discussions including persistent mechanism of extreme precipitation.

2. Data and methods

2.1. Data

The pentad mean data used in this study include the following: outgoing longwave radiation (OLR), precipitation from the Climate Prediction Center Merged Analysis of Precipitation (CMAP) (Xie and Arkin, 1997), 850 hPa and 200 hPa geopotential heights, and 850 hPa and 200 hPa winds provided by the National Center (s) for Environmental Prediction/National Center for Atmospheric Research (NCEP/NCAR). These data sets encompass 29 years (1979–2007), with global coverage on 2.50 x 2.50 grids.

Daily mean specific humidity data are utilized to derive moisture fluxes on the 850 hPa level. In addition, monthly mean sea surface temperature (SST) data on 2.00 x 2.00 grids from 1950 to 2001 (Kalnay et al., 1996) are used for examining the external forcing effect on anomalous large-scale circulations.

Although the exact definition of a drought tends to vary, precipitation below 75% of the normal value is generally defined as an indicator of a drought. Furthermore, precipitation below 25% is considered to indicate an extreme drought. Palmer (1965) devised a drought severity index based on monthly averages of temperatures and precipitation. Negative index values represent dry

spells and positive values represent wet spells, with values from -0.5 to +0.5 representing normal conditions. Values from -0.5 to -1 correspond to incipient drought, -1 to -3, moderate drought, and -3 to -4, severe drought. The values above −4.0 represent extreme drought (Barlow *et al*., 2001). In this paper, a 2.5° × 2.5° grid of the Palmer Drought Severity Index (PDSI) produced by the National Center for Atmospheric Research (NCAR), the Climate and Global Dynamics (GCD), and the Climate Analysis Section (CAS) is used as an indicator of the severity of droughts between 1960 and 2005. This PDSI consists of the monthly PDSI derived over global land areas using monthly surface temperatures (Hansen and Lebedeff, 1987) and monthly precipitation (Dai *et al*., 1997) on the basis of the moisture balance on the ground. Furthermore, the soil-holding capacity used in the PDSI was fixed to climatological maps from Webb *et al*. (1993). The PDSI used in this study has been widely applied in drought studies because of its high degree of reliability (Dai *et al*., 1998; Rajagopalan *et al*., 2000; Barlow *et al*., 2001). More details relating to constructed algorithms can be found in Dai *et al*. (1988) and Alley (1984) may be consulted for details regarding the usage and evaluation of the index.

NCEP/NCAR reanalysis monthly data (1960–2005) and the 40-yr reanalysis data (1957–2002) of European Center for Medium-Range Weather Forecasts (ERA-40) are used for the analysis of atmospheric circulation. The

climatological-pentad-mean outgoing longwave radiation (OLR) data on 2.5° × 2.5° grids are used as a proxy to represent deep convection between 1979 and 2002. Additionally, we used SST data on 2.0° × 2.0° grids to study the period of 1950–2001 (Kalnay *et al*., 1996).

2.2. Methods

2.2.1. Definition of premonsoon season

As mentioned in previous discussion, the premonsoon period is characterized by relative dryness before the onset of the East Asian summer monsoon. Spring season (March, April, and May) rainfall over Northeast Asia is smaller than that in summer, this work consider MAM averaged precipitation as a premonsoon index in this study. However, precipitation feature in May could be somewhat different from that in March and April, since the amplitude of interannual variability in May seems larger than March and April due to onset of monsoon in May over East Asian region. Indeed, some previous studies have even used May as premonsoon index, arguing composite pattern in MAM could be merely reflection of the spatial pattern of May.

According to these aforementioned, this work needs to examine whether MAM, March, April, and May is reasonable as reference of premonsoon season. Figure 1 shows time series of precipitation anomaly averaged over the region of 30°N–40°N, 110°E–140°E in premonsoon season. Each curve indicates anomaly of precipitation for March, April, May, and MAM (March, April, and May) averaged from March to May, respectively. The variation pattern of each month is similar to MAM. The standard deviations of precipitation rate in the region for

March, April, and May are 0.59 mm/day, 0.62 mm/day, and 0.68 mm/day, respectively. Thus the amplitude of variability in specific month is not represented that of premonsoon season.

For reference, anomaly composite patterns of precipitation, 850 hPa geopotential height, and 200 hPa zonal wind speed for each month for dry and wet cases are shown in Figures 2, 3, 4, 5, 6, and 7. In precipitation pattern for dry case and wet case, each month reveals well dry spell and wet spell over Northeast Asian region, respectively (Fig. 2 and Fig. 3). The 850 hPa geopotential height anomaly patterns for dry spell shown in Fig. 4 present MAM averaged anomaly pattern in Fig. 4(a), March in Fig. 4(b), April in Fig. 4(c), and May in Fig. 4(d). Dominant negative anomalies revealed over WNP region in MAM pattern show also in March, April, and May, although anomaly intensity in April is somewhat weaker than other patterns. The wet pattern of geopotential height at 850 hPa in each month is more similar to MAM pattern (Fig. 5). In the same way, anomaly pattern of MAM tilted northeastward with wave train type, is not much different from that of each month in zonal wind speed at 200 hPa (Fig. 6 and Fig. 7) except northwestward tilted in wet case. The jet core locations in all months of dry case are significantly shifted to the south compared with wet cases. Based on this analysis, this study defines March to May as premonsoon season.

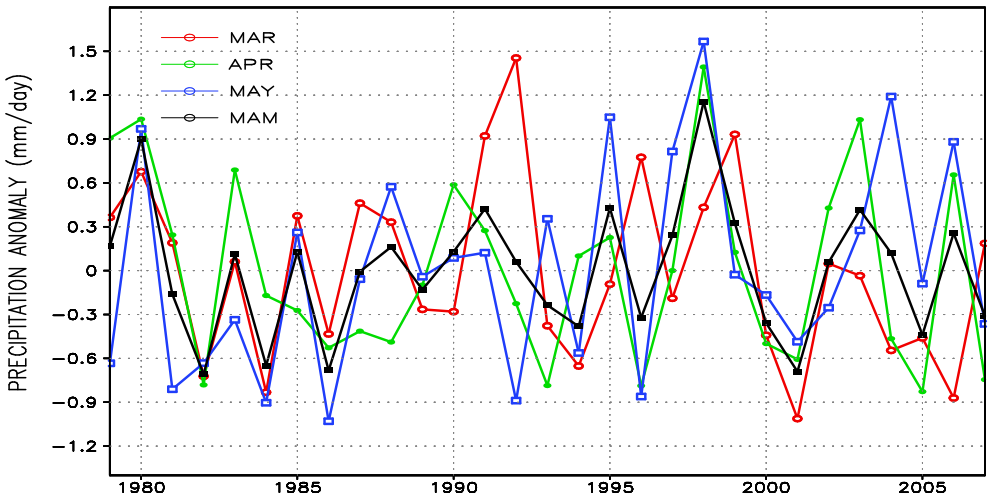

Figure 1. Time series of precipitation anomaly averaged over the region of 30°N–40°N, 110°E–140°E in premonsoon season. Each of them shows precipitation anomalies for March (red curve), April (green curve), May (blue curve), and MAM (black curve) averaged from March to May.

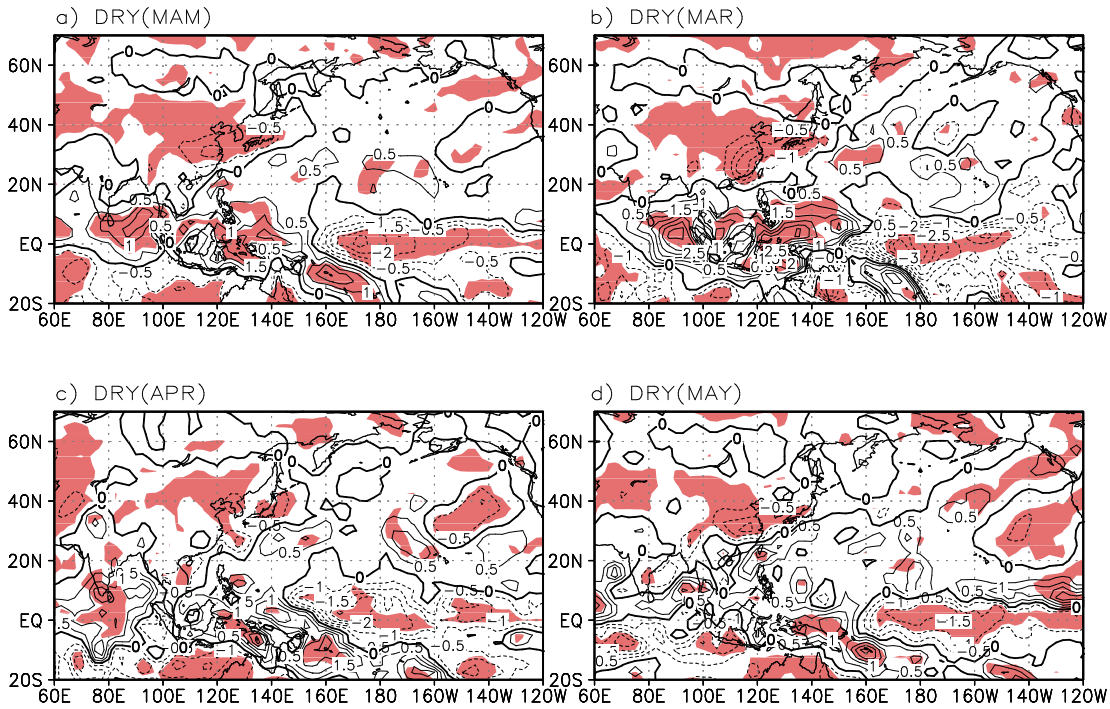

Figure 2. Composite anomalies of the precipitation for dry cases (a) March to May (MAM), (b) March, (c) April, and (d) May. The shaded areas indicate the statistical significance of the 95% confidence level. The unit of precipitation anomalies is mm/day

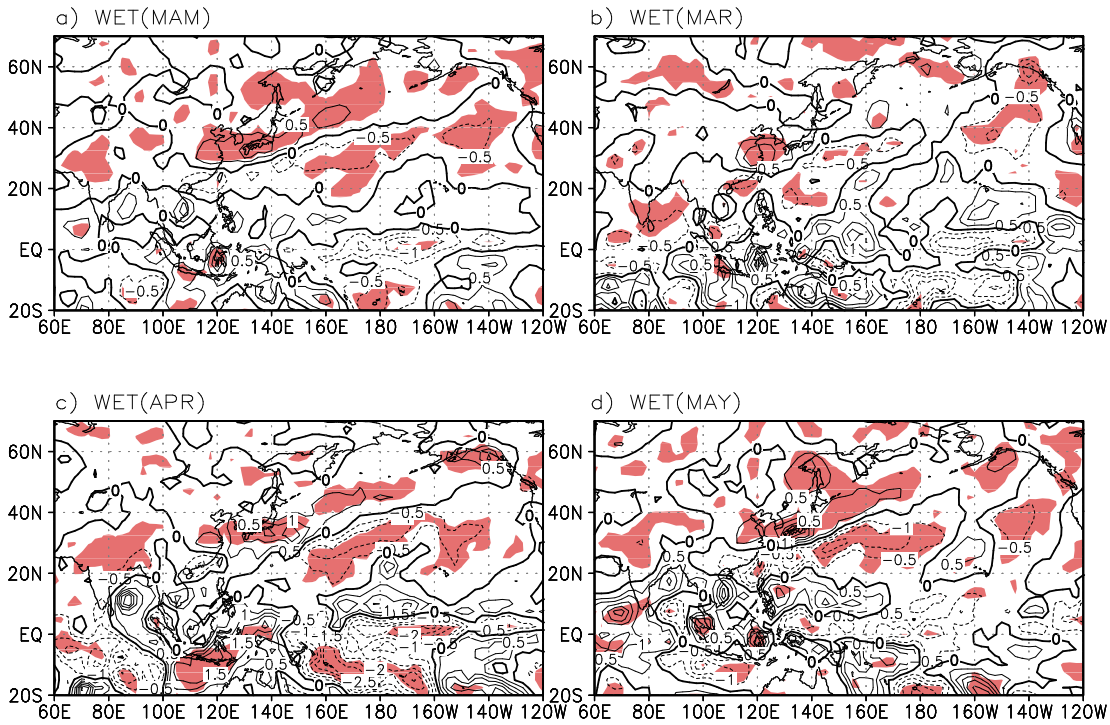

Figure 3. As in Figure 2 except for the precipitation in wet cases. The unit of precipitation anomalies is mm/day

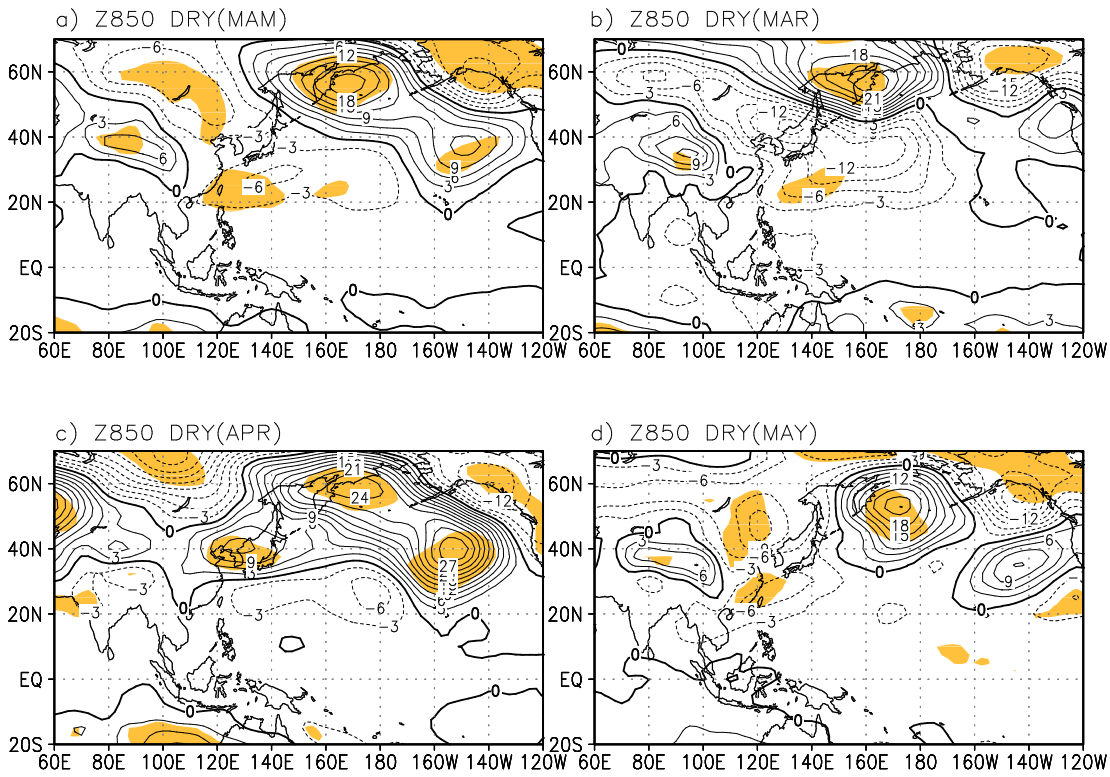

Figure 4. As in Figure 2 except for the geopotential height at 850hPa in dry cases. The units are gpm

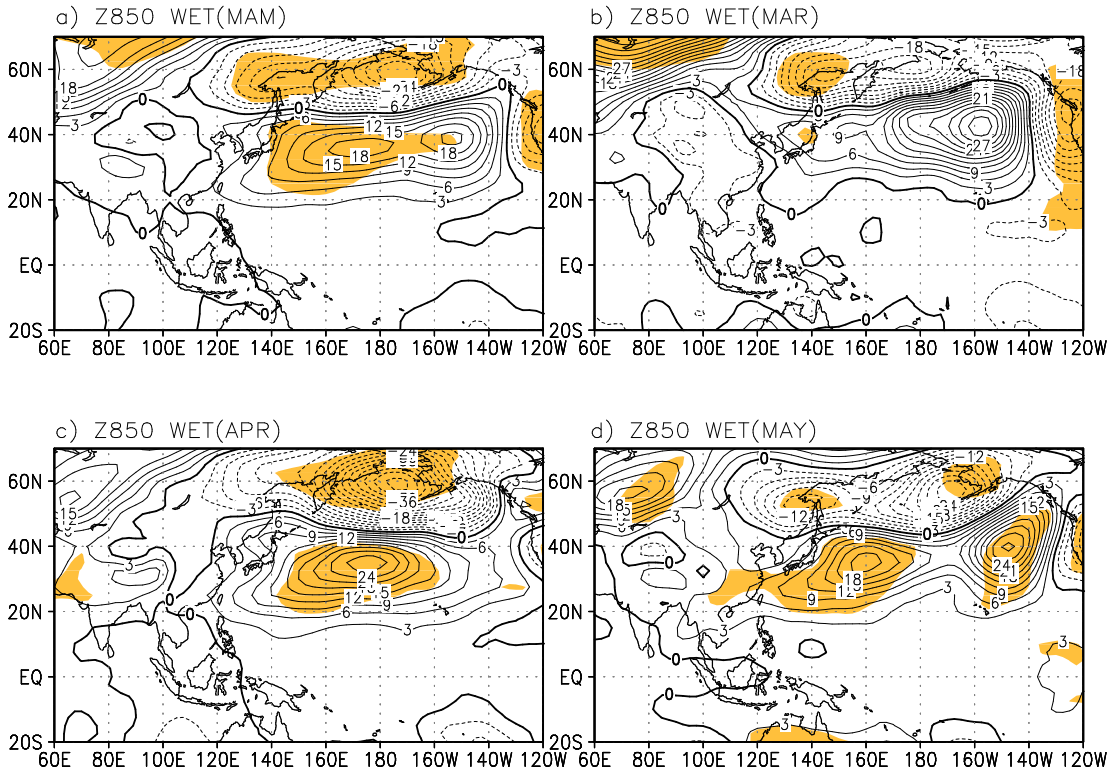

Figure 5. As in Figure 2 except for the geopotential height at 850hPa in wet cases. The units are gpm

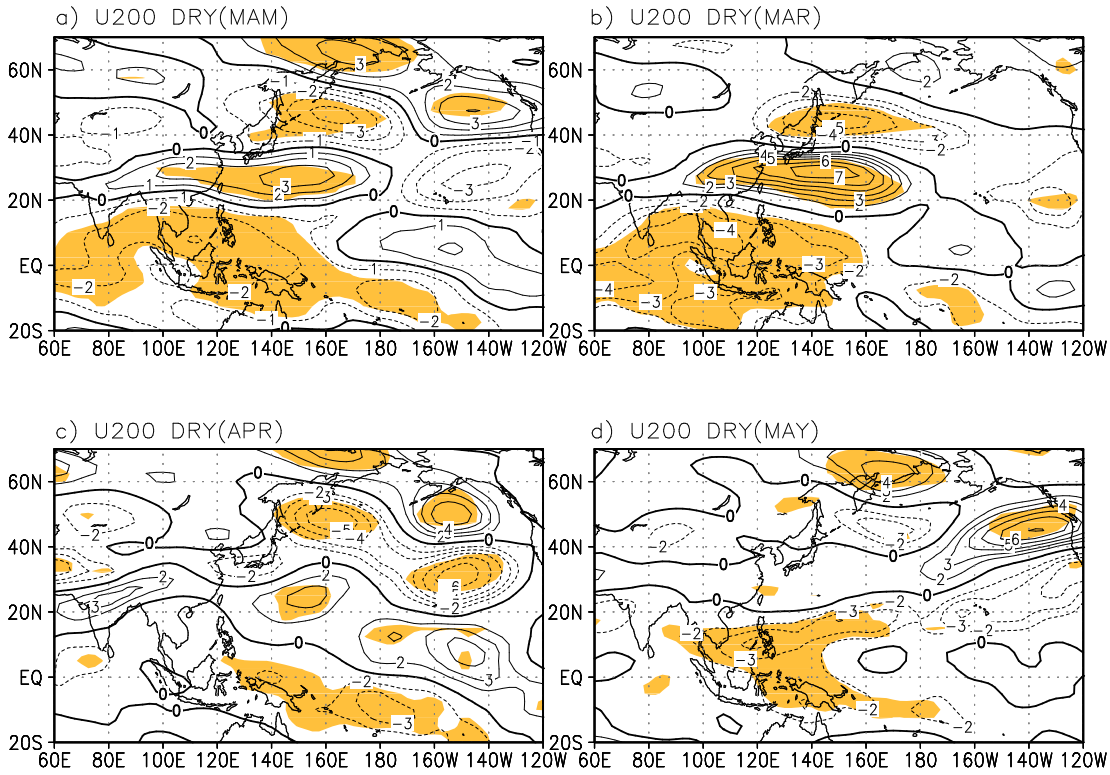

Figure 6. As in Figure 2 except for zonal wind speed at 200hPa in dry cases. The units are m/s

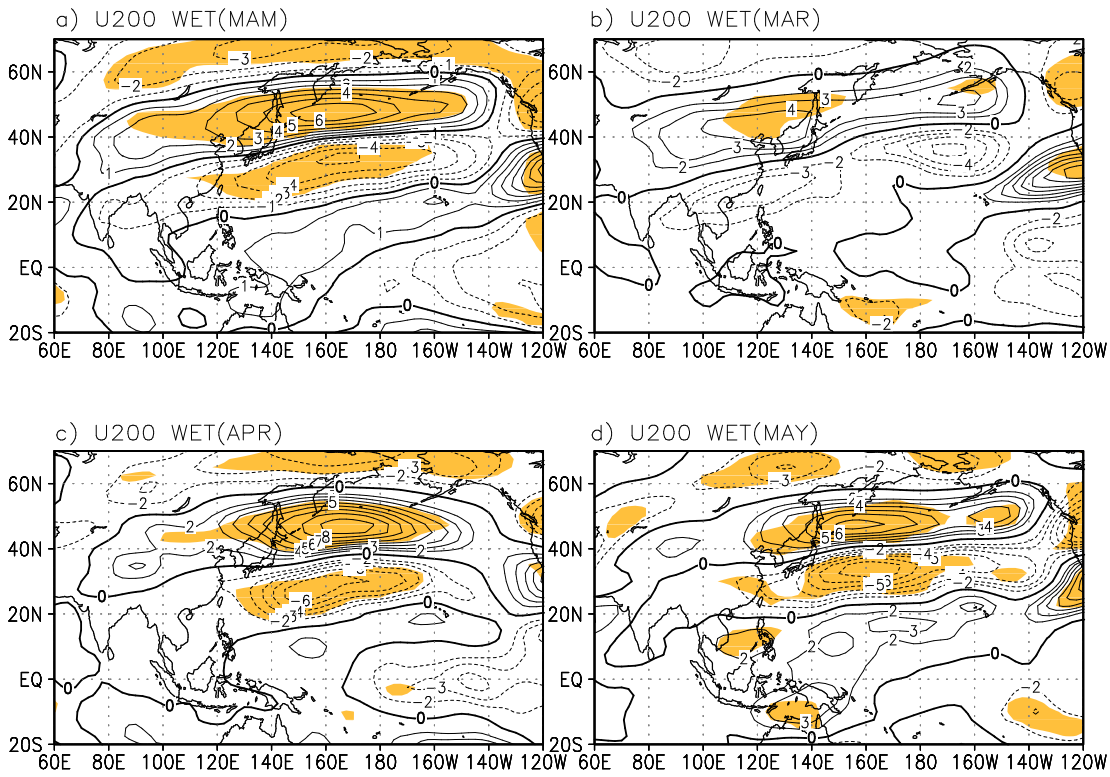

Figure 7. As in Figure 2 except for zonal wind speed at 200hPa in wet cases. The units are m/s

2.2.2. Analysis domain and selection of dry and wet years

Wang and Ho (2002) define the region of 20°N–40°N, 110°E–140°E as an EASM domain. However, we consider the EASM domain that covers only the region of 30°N–40°N, 110°E–140°E. This is because the annual variations in the climatological pentad mean precipitation in the above two domains shows very different phases, in particular from May to August (Figure 8a). The Figure 9 shows the EOF first mode of precipitation in the spring season (March to May). This eigenvector explains 45% of the total variance over the whole domain shown in Figure 9. This figure implies that the interannual variability of precipitation over the region 30°N-40°N, 110°-140°E is greatest in the northeast Asia. As seen in this figure, the large contrast in precipitation anomalies is evident between the northeast Asia and the WNP region. Therefore, the boxed domain (30°N-40°N, 110°-140°E) in Figure 9 seems to be the properly defined analysis area in our study. The difference between these two regions is due to the north-south distribution of China's summer precipitation, which has a dipole pattern: when there is a drought south of 30°N, there are floods north of 30°N (Weng et al., 1999). Dry and wet cases are defined by using the precipitation anomalies in the region encompassing 30°N–40°N, 110°E–140°E during the premonsoon period (March to May). Six dry years (1982, 1984, 1986, 1994, 2001, and 2005) and six wet years (1980, 1991, 1995, 1998, 1999, and 2003)

were selected from the lower and upper bounds, respectively, with a 0.5 standard deviation of precipitation anomaly time series (Figure 8b). More description will be discussed in section 4.

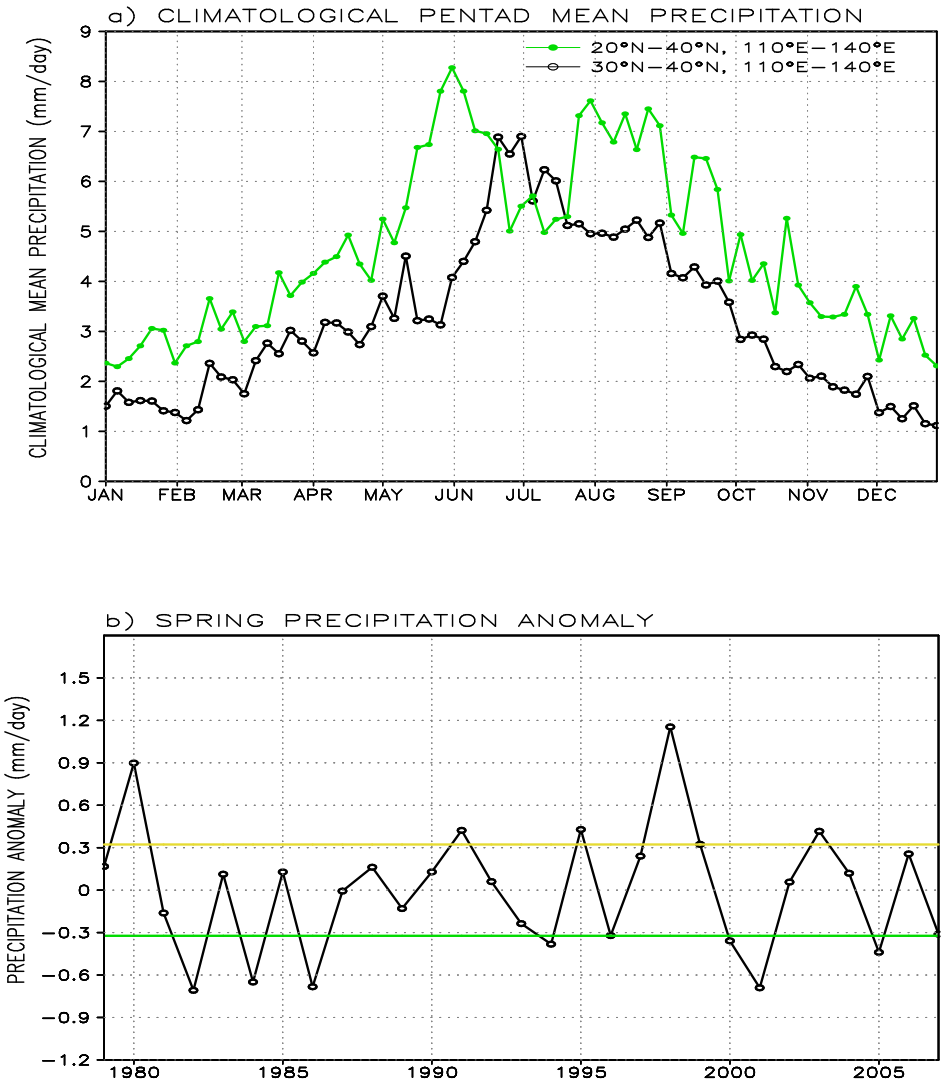

Figure 8. (a) Annual variation of climatological precipitation for the definition of the northeast Asia region, obtained from averaging over the regions of 20°N–40°N, 110°E–140°E (green curve) and of 30°N–40°N, 110°E–140°E (black curve). (b) Time series of precipitation anomaly averaged over the region of 30°N–40°N, 110°E–140°E in spring. The yellow and green horizontal lines denote ±0.5 standard deviation from the average. Units are mm/day

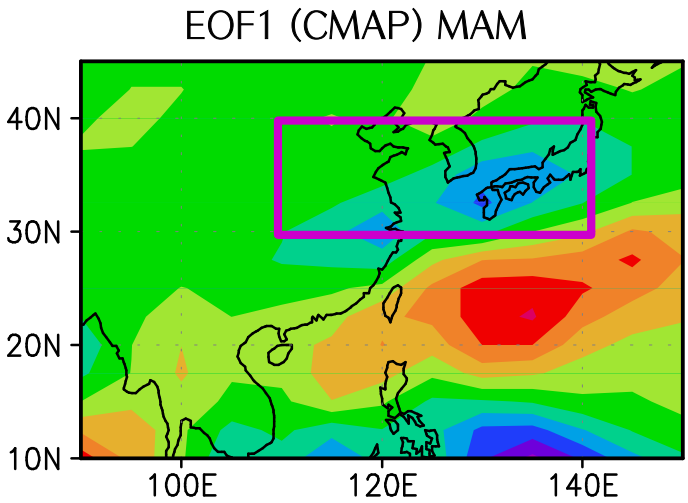

Figure 9. The first mode of the precipitation in spring time (MAM) obtained from EOF analysis. This eigenvector explains 45.25% of the total variance over the whole domain. This mode shows reversal pattern of precipitation between the region of 30°N–40°N, 110°E–140°E and the region of 20°N–30°N, 110°E–140°E.

3. Prominent features of large-scale circulation during drought

3.1 Mean fields of atmospheric circulation during boreal spring

Prior to analyzing drought phenomena, the spring mean atmospheric circulation was analyzed. The mean zonal wind speed at 200 hPa and the mean geopotential height at 500 hPa are represented in Figure 10(a). The maximum core of the EAWJ is located in the Korean Peninsula and Japan during spring and a strong upper-level atmospheric trough at 500 hPa is revealed in the core of the EAWJ at this time. In March, the maximum zonal wind speed is located between 30°N and 32°N, where the thermal wind integrated through the troposphere is at a maximum. However, the EAWJ core moves northward to 35°N in April before moving slightly further northward in May (figure not shown). The location of the rainfall band in East Asia is closely related to the meridional movement of the EAWJ (Lu, 2004). In particular, the northward shift of the EAWJ is associated with the onset of the monsoon season in East Asia (Li *et al*., 2004). The mean fields of horizontal wind at 850 hPa and the SLP for spring are shown in Figure 10(b). The mean spring SLP field displays high pressure in the northeast Asia region (30°N–40°N, 110°E–140°E) and low pressure to the north. At 850 hPa,

there is a convergence zone merged in northeast Asia through the southwesterly flow from the Bay of Bengal, the southeasterly from the Western North Pacific (WNP), and the flow from the northern part of the continent of Asia. This confluent flow may play an important role in producing rainfall in spring. The climatological mean precipitation during spring was analyzed using the pentad precipitation data (Figure 10(c)). The centre of the rainbelt is located slightly southward of the axis of the EAWJ; this is similar to the situation in summer.

CLIMATOLOGY

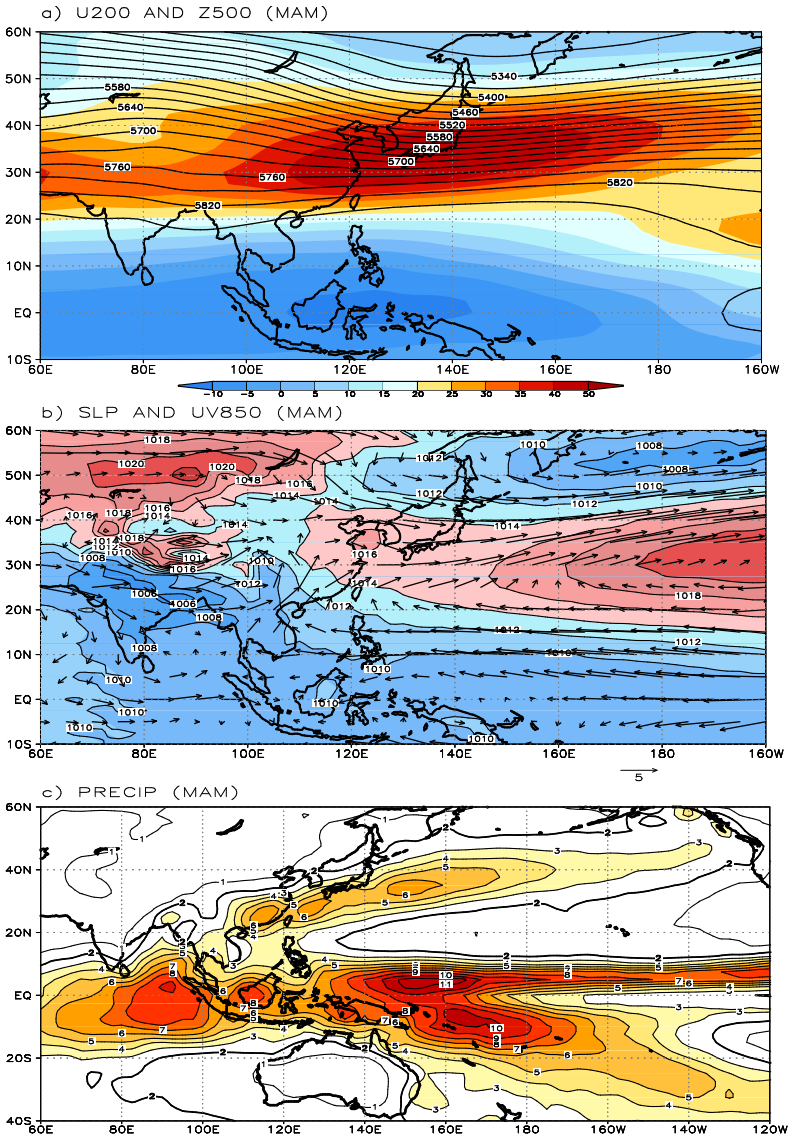

Figure 10. (a) Climatological means of zonal wind speed at 200 hPa and geopotential height at 500 hPa, (b) the climatological mean of wind vector at 850 hPa and sea level pressure, and (c) the climatological mean precipitation (mm/day) for spring (March to May, or MAM) between 1960 and 2005.

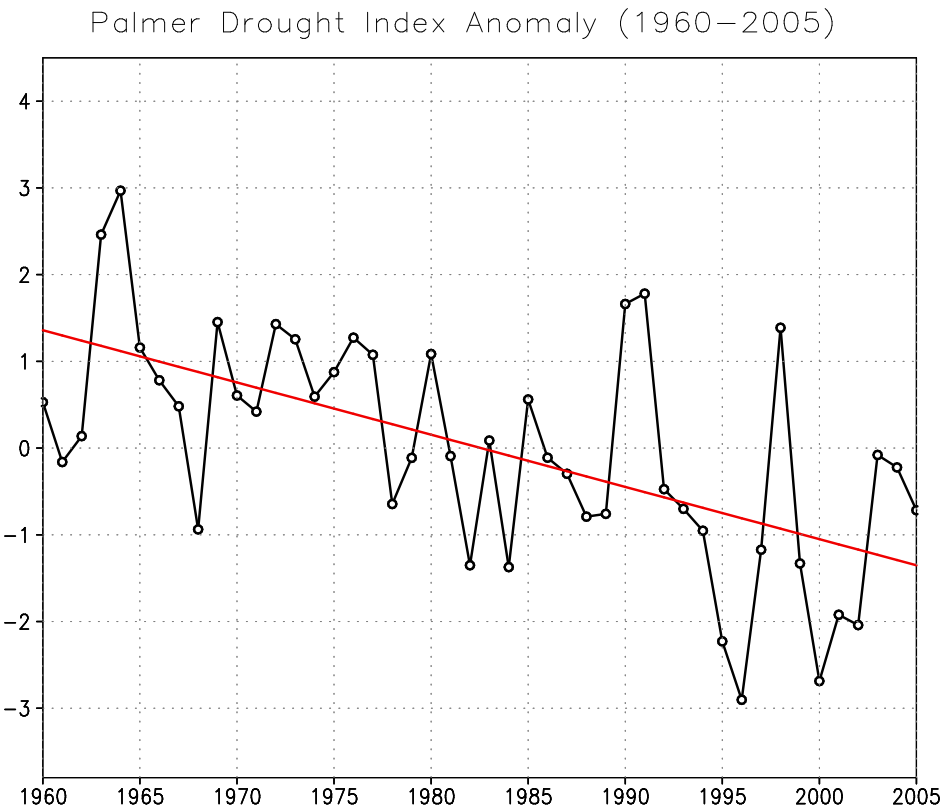

Figure 11. The MAM time series of mean PDSI over the region of 30°N–40°N, 110°E–140 °E. The values below 0.7 time standard deviation of PDSI indicate drought condition in the time series.

3.2. Definition and selection of drought years

Spring drought years in northeast Asia were selected using the PDSI anomalies. We define a drought year as a year when the average of PDSI anomalies in the region (30°N–40°N, 110°E–140°E) during springtime is less than 0.7 time standard deviations (Figure 11). According to this definition, eleven drought years between 1960 and 2005 were selected. However, patterns of precipitation anomalies must be validated in order to check whether or not these eleven drought cases have similar precipitation anomaly patterns. As a result of the validation process, 1995, 1997, and 1999 showed reversal patterns of two time series compared to other drought years. Therefore, we have excluded these three cases from the eleven selected drought years. There were eight cases (1968, 1982, 1984, 1994, 1996, 2000, 2001, and 2002) chosen as drought years. The time series of PDSI anomalies displays a decreasing trend from 1960 onward. In particular, five of the eight drought cases occurred after 1990; this may be associated with the variations in atmospheric circulation in Asia since the 1990s (Kwon *et al*., 2005, 2007). Interestingly, this decreasing trend in the PDSI anomaly time series is very similar to that in the time series of temperature anomalies in the upper troposphere over 30°N–40°N, 110°E–125°E, as shown in Xin *et al*. (2006). This similarity implies that the PDSI is closely related to the

temperature in the upper troposphere. The high correlation coefficient (0.53) between the PDSI and the temperature of the upper troposphere supports this implication.

3.3. Atmospheric circulation anomalies during drought years

The composite of geopotential height anomalies in the upper levels is shown in Figure 11. The geopotential height anomalies at 300 hPa, 500 hPa, and 850 hPa exhibit a strong cyclonic circulation over the Korean years Peninsula and Japan, and an anticyclonic circulation to the north of this region. These cyclone–anticyclone the anomaly patterns from upper level to the lower level indicate a strong barotropic structure. As shown by Bar-low *et al*. (2001), this barotropic structure is associated with drought through the suppression of the moisture flux from the WNP region and the divergence related to these dipole patterns. The weakening of WNPSH at 850 hPa is significant (Figure 12(c)) and the westward shifting of negative height anomalies is dominant as shown in Figure 13(a) and Figure 13(b). The Figure 13 shows the climatology of spring (MAM) and dry MAM at 850hPa height from 1979 to 2007. The shaded areas denote statistical confidence levels of 95% and the thick contours indicate contour levels of 1520 and 1540. The 1520 and 1540 contours are significantly retreated eastward by about 6° longitude in dry MAM compared to those of climatology. The statistically confident areas (shadings) over the region of 10°N-30°N, 110°E-140°E imply the above mentioned features (Figure 12). Thus, the WNPSH in dry cases weakened compared with climatology.

This height anomaly pattern at 850 hPa indicates that the moisture flow from the Indian Ocean and the Western Pacific is significantly reduced and that this anomaly pattern plays a role in suppressing the moisture flow. Therefore, the weakened WNPSH is associated with spring droughts in the Korean Peninsula, Japan, and Southeast China. The WNPSH also plays an important role, along with the north–south shift of the westerly jet stream, in determining summer monsoon rainfall anomalies in East Asia.

To examine the relationship between the moisture flow and the WNPSH as it relates to spring droughts, we performed a composite analysis of wind vector anomalies at 850 hPa and precipitation anomalies. Figure 14 displays horizontal wind vector anomalies at 850 hPa (arrow) and precipitation anomalies (contour) during drought years. There is clearly a negative anomaly with regard to the precipitation over the Korean Peninsula, Japan, and China (30°N–45°N, 110°E–140°E). The positive precipitation anomaly is zonally elongated and located to the south of the Korean Peninsula and Japan (20°N–30°N, 125°E–180°). At 850 hPa, there are distinctive anticyclonic circulation anomalies in the region 37°N–60°N, 125°E–180° and cyclonic circulation anomalies in the region of 18°N–33°N, 125°E–180°. This anomalous wind vector pattern is opposite to the climatology of the SLP and the 850-hPa wind vector (Figure

10(b)) and is responsible for the suppression of the moisture flow from the south. The cyclonic circulation in the south of Korea and Japan indicates the weakening of the WNPSH. A significant northerly wind is found, along with negative precipitation anomalies, over the Southeastern China (18°N–32°N, 110°E–120°E) (Figure 14). This is contrary to the southwesterly wind pattern from Southeast China, as shown in Figure 10(b).

The anomalous rainfall band during spring drought years is located along 20°N–30°N (Figure 14), while the rainfall band in the climatology develops from 15°N to 40°N along the western edge of the WNPSH to the south of the Korean Peninsula. This indicates that the rainfall band in spring drought years does not move northward to the northeast Asian region but remains south of 30°N. Thus, spring droughts seem to occur in the Korean Peninsula, Japan, and Eastern China; negative precipitation anomalies are dominant over northeast Asia. There is a strong but positive anomaly near the Philippine Sea (10°S–15°N, 120°E–140°E), displaying a pattern that is opposite from that over northeast Asia.

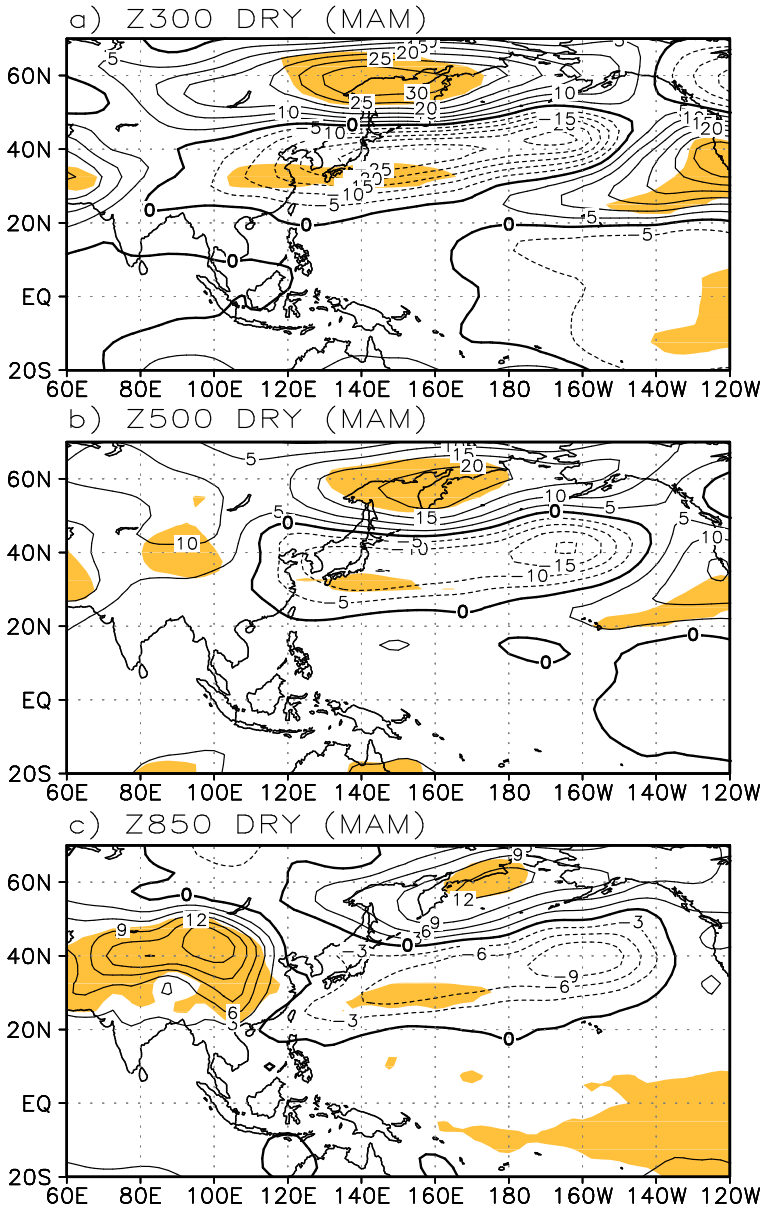

Figure 12. The geopotential height anomaly composite for spring drought years at (a) 300 hPa, (b) 500 hPa, and (c) 850 hPa. The shaded areas denote the regions that are statistically significant (95%).

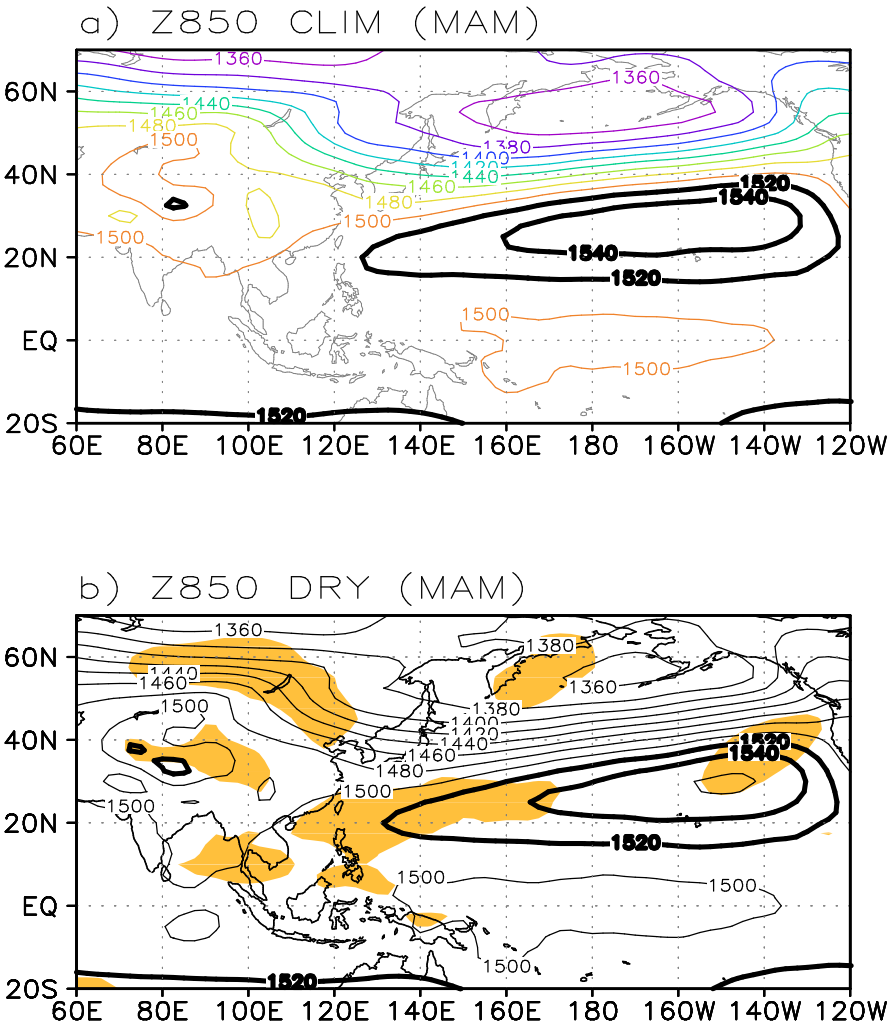

Figure 13. The climatology of spring (MAM) and dry MAM at 850hPa height from 1979 to 2007. The shaded areas denote statistical confidence levels of 95% and the thick contours indicate contour levels of 1520 and 1540.The geopotential height anomaly composite for climatology at (a) 850 hPa and (b) for drought years at 850 hPa.

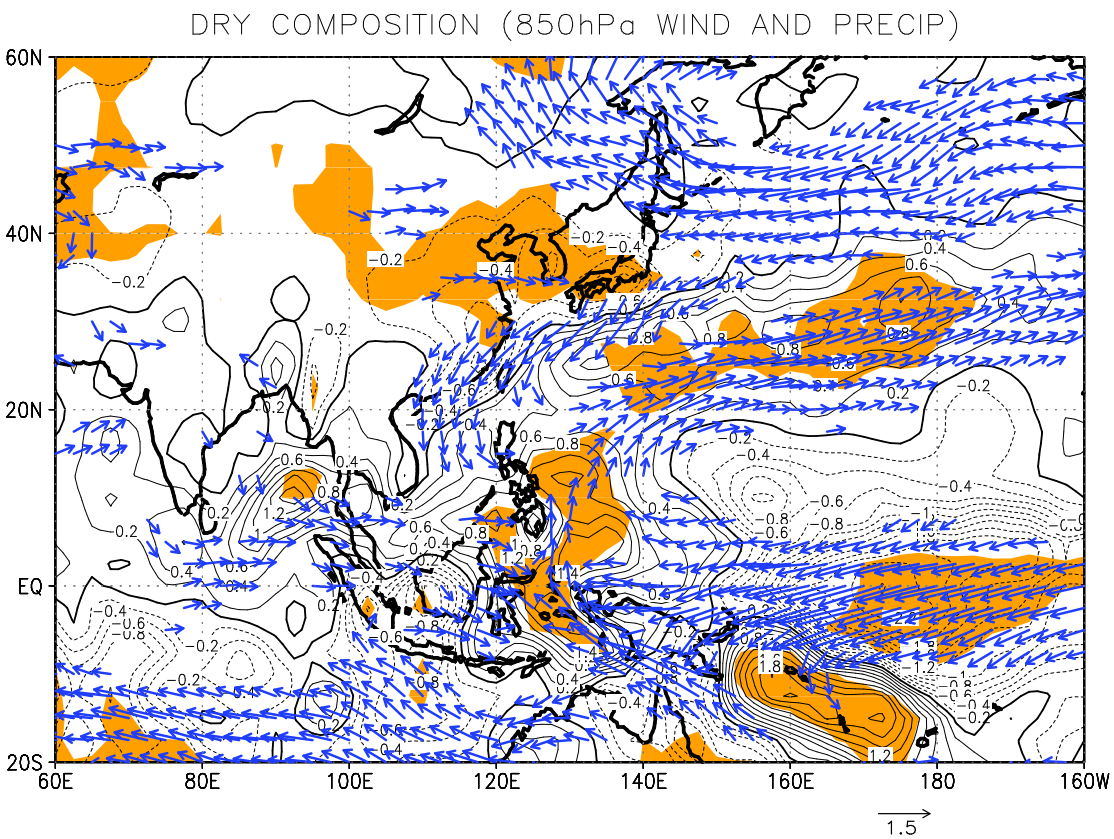

Figure 14. The composite anomaly map of wind vectors (arrow) at 850 hPa and precipitation (contour) for drought years. The shaded areas denote the regions that are statistically significant at the 95% confidence level for precipitation.

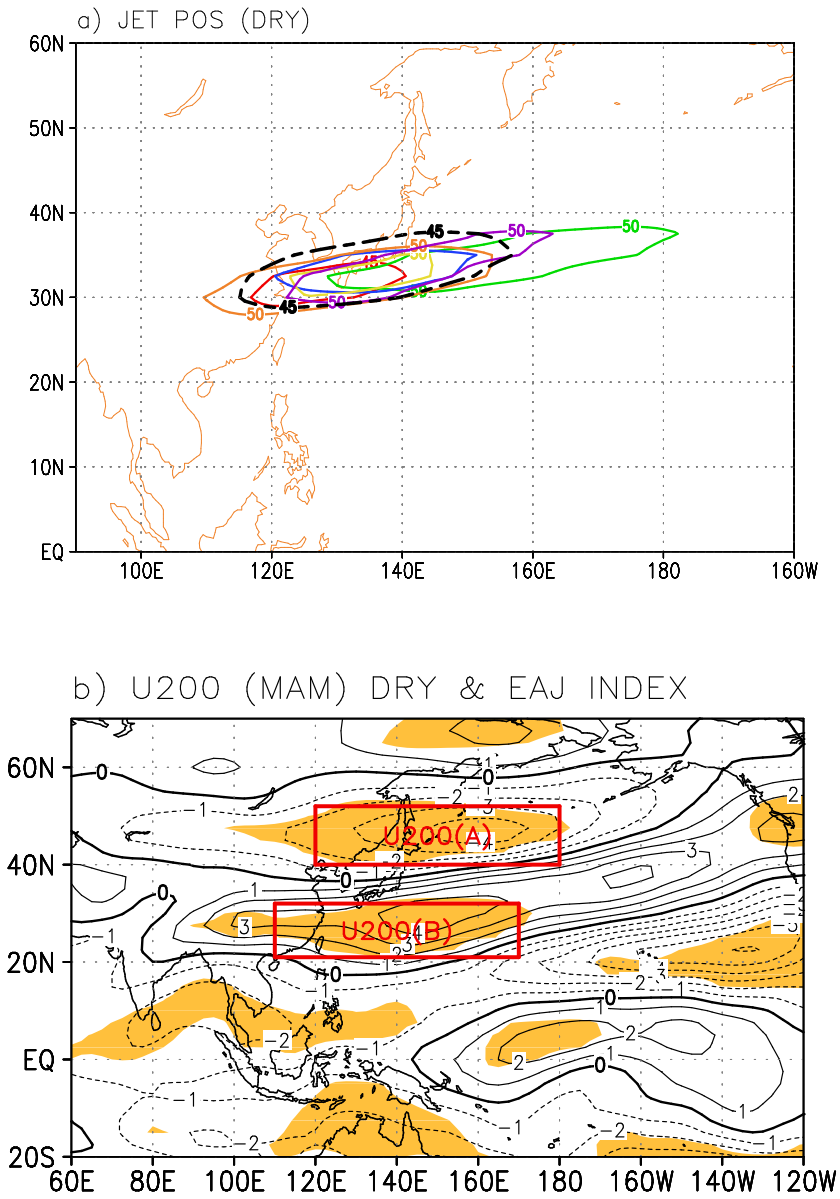

Figure 15. (a) The contours representing the EAJ core at 200 hPa in mean (dashed line) and in individual drought years (solid lines), and (b) the composite of zonal wind speed anomalies at 200 hPa for drought years. The contour interval is 1 m/s in (b). The statistically significant regions (95%) are shaded.

Figure 15(a) displays the cores of the maximum zonal wind speed at 200 hPa in the spring mean and individual drought years. The thick dashed line represents the jet core of a 46-year (1960 to 2005) spring mean of the zonal wind at 200 hPa and the other solid contours represent those of individual years. The solid contours (jet cores in drought years) are displaced southward by approximately 3°N–5°N latitudes, compared to that of the 46-year spring mean. The composite of the zonal wind anomaly at 200 hPa for the spring drought years is shown in Figure 15(b). The anomalous positive zonal wind speed band located at 25°N implies a southward shifting of the jet core and the location of the anomalous positive maximum of the zonal wind speed almost corresponds with that of the precipitation (Figures 14 and 15(b)). The jet stream axis is closely associated with the frontal zone where the meridional temperature gradient is at its highest and corresponds with the rainfall band. The average temperature anomalies in the troposphere (1000 hPa–300 hPa) are shown in Figure 16. This figure reveals that the mean meridional temperature gradient is clearly reduced (negative anomalies) over the Korean Peninsula, Japan, and Eastern China (30°N–45°N, 120°E–160°E). There are positive anomalies to the north and south of the above-mentioned region. The relationship between upper-level zonal wind anomalies (Figure 15(b)) and temperature anomalies (Figure 16) can be explained by considering the thermal wind relationship. The

location of the maximum positively anomalous zonal wind speed over the WNP region is consistent with the most negative meridional temperature gradient. Meanwhile, the location of the most negative anomalous zonal wind speed to the north of the positive maximum is also consistent with temperature fields.

3.4. Teleconnection between droughts and SSTs

3.4.1. SST and OLR anomalies

It is important to understand why the rainfall band did not progress northward to 35°N from the WNP but rather remained in the region 20°N–25°N. Furthermore, it is imperative that we examine what forces cause the change in atmospheric circulation anomalies. Anomalous SSTs and convection in the Pacific, due to the altered atmospheric heating in the tropics, probably influence large-scale circulation such that the quasi-stationary planetary waves, the jet stream location, and the associated storm track (Trenberth and Guillemot, 1996) reflect changes in the seasonal movement of the WNPSH (Wu and Wang, 2000).

Figure 17 displays a composite of SST and OLR anomalies for the spring drought years. The SST and OLR anomalies differ greatly in the Western Pacific (10°S–20°N, 120°E–160°E). That is, negative OLR anomalies over positive SST anomalies appear over the tropical Western Pacific. However, in the subtropical Western North Pacific, negative OLR anomalies appear over negative SST anomalies. It is likely due to the difference of air–sea interaction between the tropical Western Pacific and the subtropical Western North Pacific. The SST and OLR anomaly patterns, shaded as statistically significant at the level of 95% (Figure 17), are very similar to the spring precipitation anomaly pattern shown in

Figure 14. It should be noted that the areas of strong convection (negative OLR anomaly) and warm SST (positive SST anomaly) in the tropical Western Pacific (Figure 17) correspond to the positive rainfall anomaly pattern shown in Figure 14 but the areas of strong convection and cold SST are associated with the positive rainfall anomaly pattern in the subtropical Western North Pacific. From the results of this analysis, we may infer that the strong anomalous convection over the tropical Western Pacific leads to moisture modulations through an anomalously latent heat release. The moisture anomalies can also lead to considerable variations in vertical motions and precipitations. On the other hand, circulation anomalies associated with negative OLR and positive precipitation anomalies can lead to negative SST anomalies in the subtropical Western North Pacific.

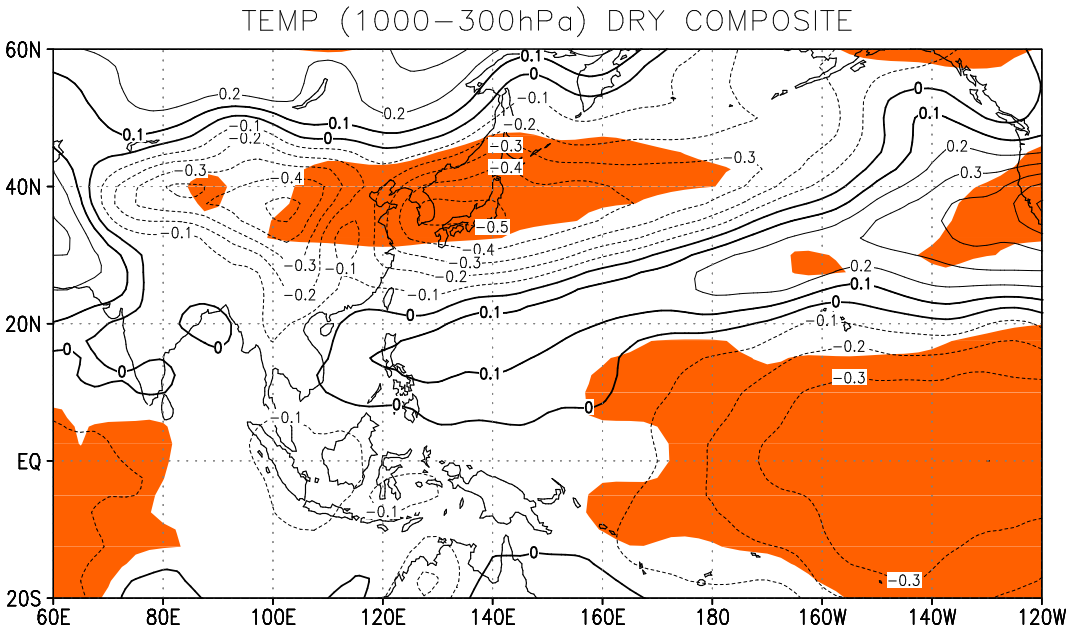

Figure 16. The composite of the vertical-averaged anomalous temperature (1000 hPa–300 hPa) for spring droughts. The shaded areas denote the regions that are statistically significant at the 95% confidence level for temperature.

3.4.2. Definition of the EAWJ index

In the previous subsection, we analyzed the characteristics of SST anomalies and associated anomalous convections for spring drought years, finding that the SST anomalies, especially in the Western Pacific, seemed to cause the displacement in the jet stream location through substantial changes in vertical motions in the tropics. In order to develop a clearer understanding of the ways in which the SST affects large-scale atmospheric circulation for drought years, we must define the EAWJ index. The dynamic relationship among the SST anomalies, the change in the EAWJ location, and associated rainfall anomalies can be analyzed through the EAWJ index, an examination of composite maps of the vertical velocity along 125°E–135°E, and a discussion of the meridional wind at 850 hPa.

The EAWJ index is defined as the area-mean difference [U200 (A) (40°N–51°N, 120°E–180°)] minus [U200 (B) (21°N–32°N, 110°E–170°E)] of the composite of spring zonal wind speed anomalies at 200 hPa for the period of 1960–2005 between the north and south of Korea and Japan (Figure 15). In Figure 15, the region of 40°N–51°N, 120E–180° (the north of Korea and Japan) indicates negative anomalies, while the region of 21°N–32°N, 110°E–170°E (the south of Korea and Japan) indicates positive anomalies in upper-level zonal wind anomalies for spring drought years. Indeed, these results show a north–south

dipole pattern. Therefore, the difference between U200 (A) and U200 (B) implies a change in the EAWJ core location; the negative deviation value indicates that the EAWJ core location is displaced southward, while the positive deviation value signifies a northward shift of the EAWJ core location.

In order to compare the EAWJ index with temperature at 300 hPa, precipitation, and PDSI for drought years, correlation coefficients were calculated using values obtained from the time series of the area-mean anomaly in the region of 30°N–40°N, 110°E–140°E. The correlation coefficient between the EAWJ index and the upper-level (300 hPa) temperature anomaly is as high as 0.71, while the correlation coefficient between the EAJ index and the precipitation over northeast Asia is 0.69 and the correlation coefficient with the PDSI is 0.47. These significant correlation coefficients imply that the EAWJ index could be used to measure the intensity of spring droughts.

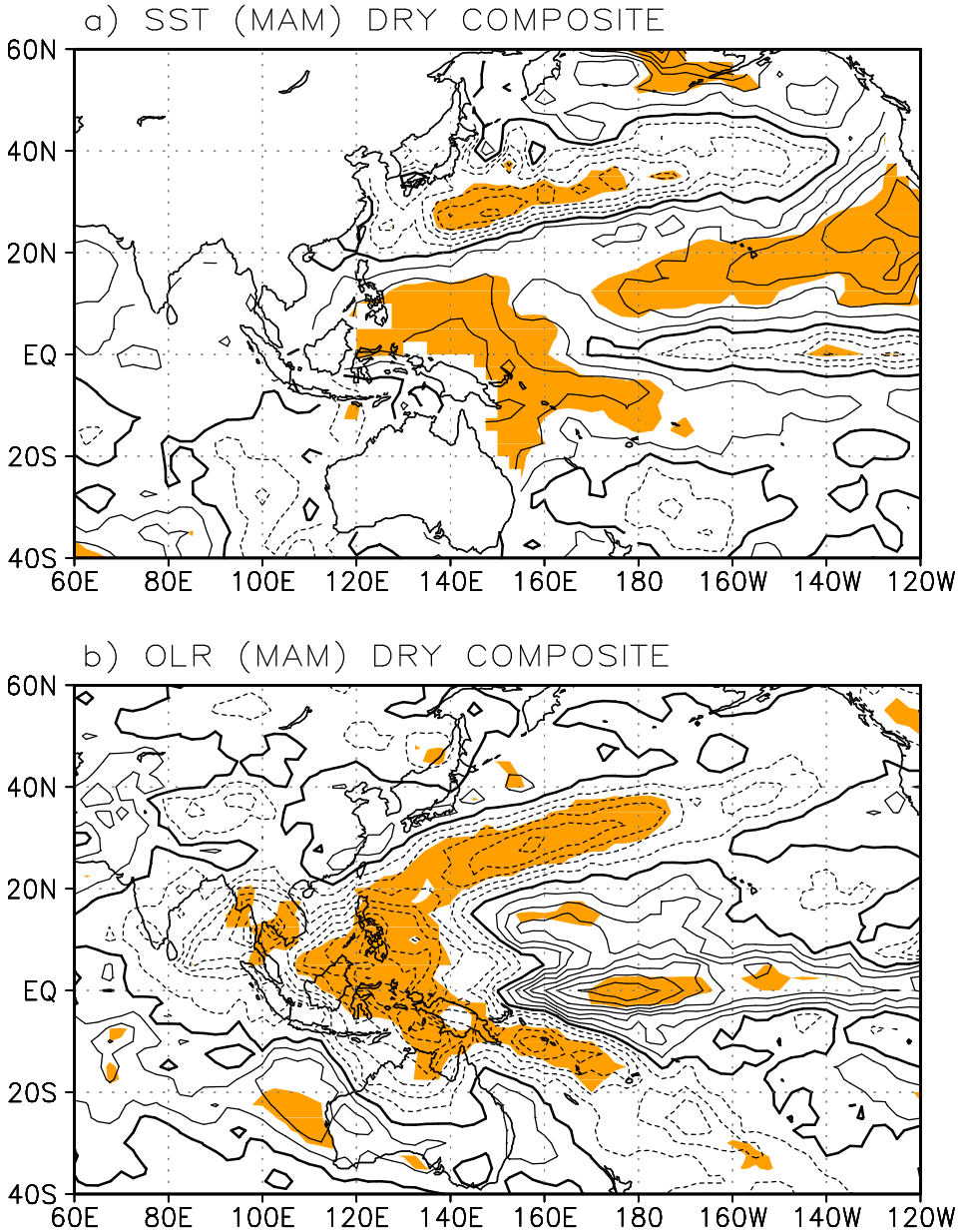

Figure 17. The composite maps of (a) SST anomalies and (b) OLR anomalies for spring drought years. The shaded areas are statistically significant (95%). The contour interval of the SST anomalies is 0.1 °K, while that of the OLR anomalies is 0.2 W/m^2.

3.4.3. The relationship among the EAWJ index, SST, and precipitation

The correlation between the EAWJ index and SST anomalies during springtime is presented in Figure 18(a). The SST anomalies and the EAWJ index exhibit a negative correlation of about −0.3 near the Philippine Sea, which means that there is out of phase between two elements; that is, when the EAWJ is located in the south (negative index), the strong convection (positive SST anomalies) occurs in the Western Pacific (0°–15°N, 120°E–145°E). On the basis of the above assertion, this study confirms that anomalous SST convection in the Western Pacific leads to atmospheric circulation (i.e., changes in the location of the jet stream).

Another noticeable feature exhibited in the correlation map between the EAWJ index and the SST anomaly is a clearly positive correlation in the region of 20°N–40°N, 125°E–180°. This positive correlation indicates that the jet core location is concurrently displaced southward when the SST lowers. This cold SST to the south of Japan (25°N–35°N, 130°E–160°E) is made up of a dipole pattern with the warm SST located in the Western Pacific (around the Philippine Sea: 0°–20°N, 120°E–160°E). This prominent dipole pattern in SST anomalies is also represented in drought years (Figure 17(a)) and is consistent with the surface air temperature anomaly pattern (not shown), indicating negative anomalies in

the south of Korea and Japan (20°N–32°N, 125°E–160°E) and clearly positive anomalies around the Philippine Sea (0°–18°N, 115°E–150°E). The surface temperature anomaly pattern can be explained as a primary dynamics of the SST anomaly pattern, as shown in Figure 18(a), and is closely associated with the north–south displacement of the EAWJ (Figures 15(b) and 16). Figure 18(b) shows a very high positive correlation coefficient of 0.6–0.7 between the EAWJ index and the precipitation over the Korean Peninsula and Southern Japan (30°N–45°N, 90°E–140°E). Furthermore, the figure shows a correlation coefficient of −0.4 to −0.6 over the region of 20°N–30°N, 110°E–140°E. This correlation is consistent with the composite pattern of precipitation anomalies for spring droughts, indicating that the southward movement of the EAWJ seems to be directly related with spring precipitation anomalies in northeast Asia, the Korean Peninsula, and Japan.

From the above observation, we may infer that the anomalous Western Pacific convection and the associated moisture modulations give rise to an anomalously latent heat release, which in turn causes considerable variations in vertical motions and the associated large-scale circulation. Figure 19 displays the vertical cross section of the p-velocity and the meridional wind along 120°E–140°E during spring drought years. It is important to note the upward motions from the equator to 25°N, where anomalous convections (warm SSTs)

are strong (Figures 17 and 18(a)). Likewise, it is important to note the strong downward motions over 30°N–40°N, where the spring droughts occur (Figures 14 and 18(b)). The anomalous descending motions over 30°N–40°N in drought years correspond to Figure 18(b). Furthermore, Figure 18 provides a clearer understanding of how the vertical motion of the atmosphere affects the location of the EAWJ and the WNPSH intensity during spring droughts. That is, the anomalous ascending motion of warm SST anomalies in the Western Pacific (0°–25°N) leads to a descending motion in northeast Asia (30°N–40°N) due to Hadley circulation. For this reason, spring droughts occur in northeast Asia. Another prominent feature is the strong northerly flow at the lower level of the latitudinal band (18°N–32°N). This anomalous northerly flow is nearly consistent with the strong zonal wind vector anomaly at 850 hPa in Southeast China, as shown in Figure 14. Consequently, it was found that the both the WNPSH and the EAWJ play a role in controlling the moisture flux that moves into northeast Asia during spring droughts. Furthermore, the SST anomaly in the Western Pacific affects the change in intensity of the WNPSH and the EAWJ.

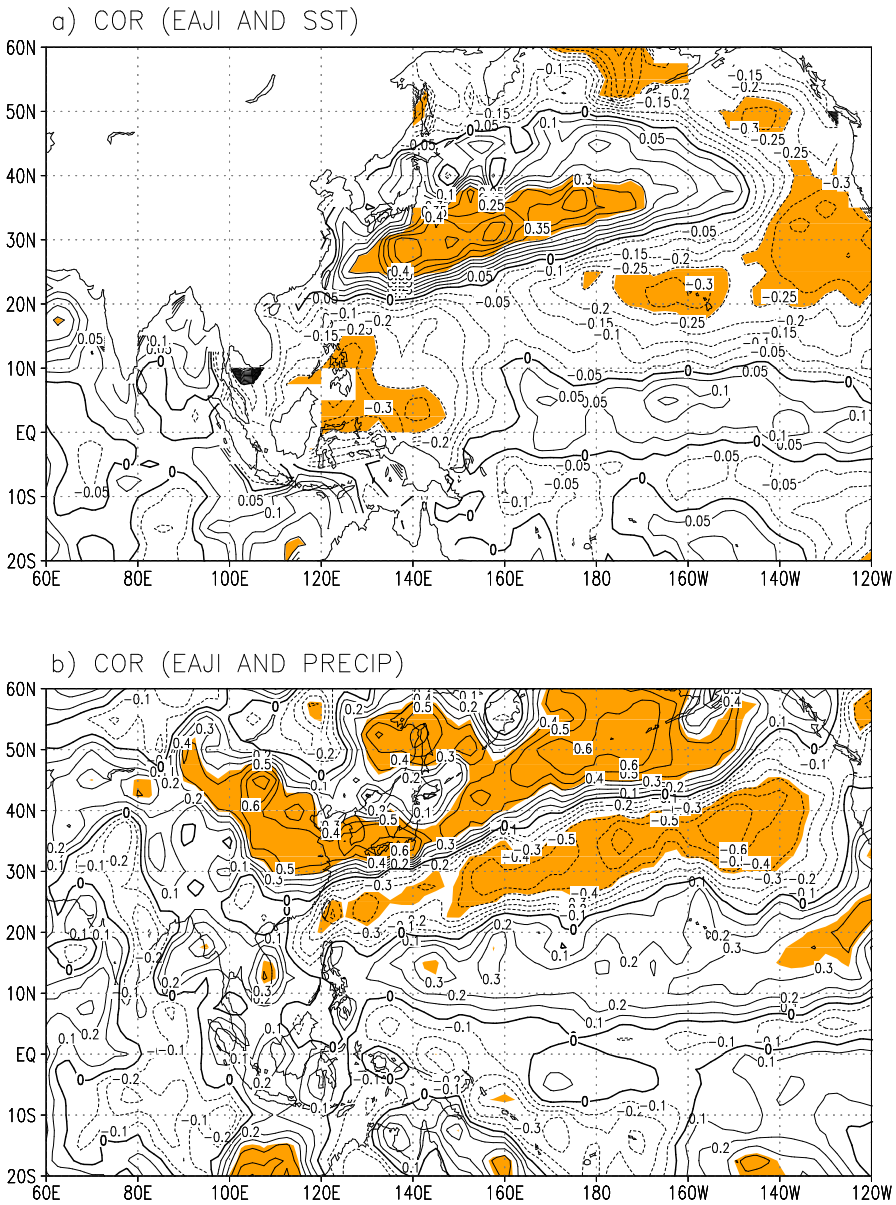

Figure 18. (a) The correlation coefficients between EAWJ index and SST anomalies, and (b) the correlation coefficients between EAWJ index and precipitation anomalies. The shaded areas denote the regions that are statistically significant (95%).

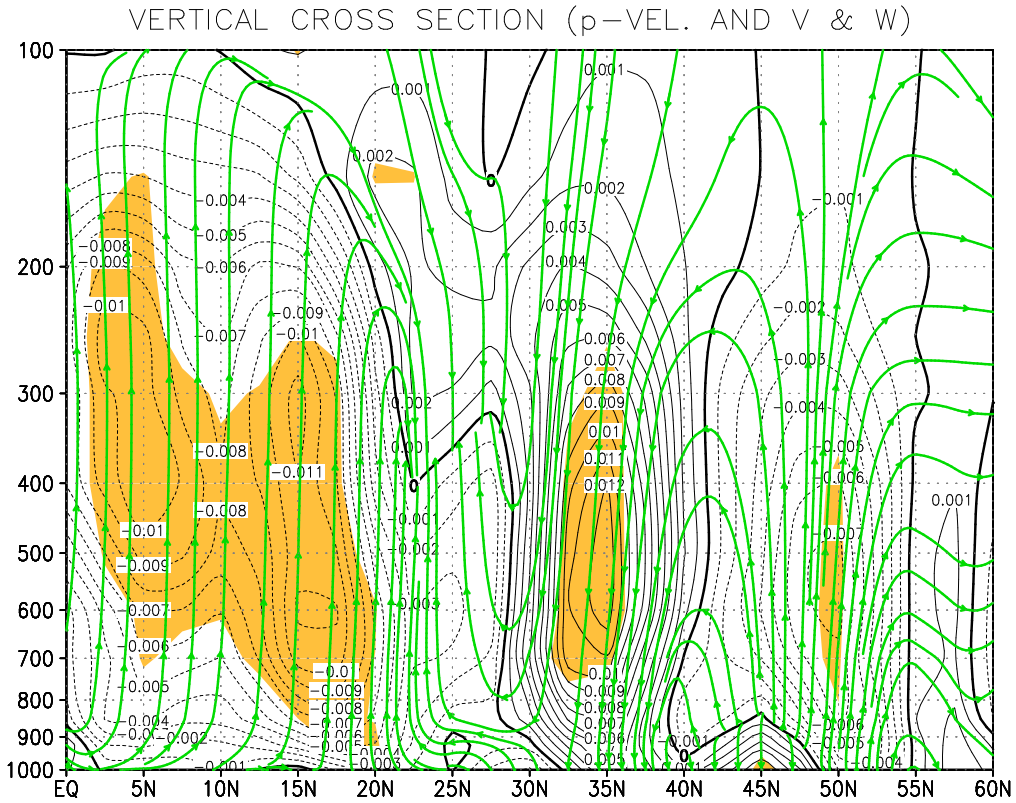

Figure 19. A latitude-height cross section of the p-velocity and meridional wind speeds along 120°E–140°E in spring drought years. The contour represents omega velocity anomalies. The shaded areas denote the regions that are statistically significant (95%).

4. Characteristics of anomalous Atmospheric Circulations in the spring and summer

4.1 Selection of Dry and Wet Cases

In order to examine the anomalous large-scale circulations of the premonsoon and the subsequent summer monsoon periods, we define dry cases and wet cases based on the premonsoon precipitation anomaly from March to May (MAM), as described in section 2. Composite analysis was performed for the examination of the relationship between atmospheric large-scale circulations in the spring and those in the summer for dry and wet cases. Discussion of this analysis will focus on the dry cases, because wet cases basically have the opposite features.

The composite precipitation anomalies over the region of 30°N–40°N, 110°E–140°E for the dry and wet cases and their three-pentad running means are shown in Figure 20. These two composites of precipitation anomalies show clear reversal patterns, especially from March (Pentad 13, i.e., P13) to July (P40). This period covers the onset and retreat of the summer monsoon over East Asia. Most notably, the composite of dry cases shows an abrupt decrease of precipitation in late June.

4.2. Precipitation Anomalies

Figure 21 shows the composite of precipitation anomaly distribution for spring and summer for the dry and wet cases. In the dry springtime, there are negative anomalies over the northeast Asian region, whereas positive anomalies exist near the Philippines. In particular, a strong rainfall area in the spring is located to the south and southeast of the Philippines (10°S–15°N, 110°E–150°E), and this rainfall region seems to be displaced northward in the summer. It is noted that the precipitation anomaly pattern continues from spring to summer in the dry cases (Figures 21a and 21c).

On the other hand, positive anomalies of precipitation are revealed in the Korean peninsula and southern Japan in both the spring and the summer of the wet cases, whereas negative precipitation anomalies are evident east of the Philippines (5°N–15°N, 130°E–160°E) in the summer of wet cases (Figures 21b and 21d). The precipitation anomaly distributions for wet cases show almost completely opposite patterns of those for dry cases, especially in the summer.

On the basis of the persistence of the spatial pattern during the spring and summer, the relationship between spring and summer rainfall anomalies from 1979 to 2007 has been calculated. Figure 22 presents correlation coefficients between the precipitation anomaly time series over the region of 30°N–40°N,

110°E–140°E in the spring and the precipitation field in the summer. The high positive correlation coefficient of over 0.5, which is significantly over the 95% confidence level, applies to Korea, Japan, and northeast China. This positive correlation between both seasons supports the persistence of spring and summer precipitation anomalies.

4.3. Geopotential Height Anomalies at 850 hPa

The WNPSH is one of the major large-scale circulation systems that affect East Asian summer monsoon rainfall. Previous studies have indicated that the western subtropical ridge plays an important role in determining the onset and withdrawal of the summer monsoon (Lau and Li, 1984). The summer monsoon season, called Changma in Korea, is known to be associated with the penetration of the subtropical Pacific high to south of the Korean Peninsula (Kang et al., 1999). To examine the effect of the WNPSH on precipitation over northeast Asia in the premonsoon and summer monsoon seasons, geopotential height fields at 850 hPa are analyzed.

The composites of the geopotential heights at 850 hPa are shown in Figure 23. A negatively anomalous circulation indicating a weakening of the WNPSH is exhibited over the western North Pacific in the spring of dry cases (Figure 23a). The negative anomaly center over the western North Pacific (WNP) region moves southward and the anomaly intensity is enhanced in the summer of dry cases (Figure 23c). In addition, significant positive height anomalies exist over northeast Asia in the summer. This positive height pattern, with the weakened WNPSH, is associated with the summer drought over northeast Asia, which acts to suppress the moisture supply from the Indian Ocean and the

western flank of the western subtropical high, thereby leading to the suppression of rainfall over Korea and Japan (Park and Schubert, 1997).

On the other hand, an enhanced subtropical high is dominant in the spring of wet cases (Figure 23b). Also, strong negative height anomalies develop to the north of this subtropical high. Interestingly, the Korean peninsula and Japan are located in a confluent zone in the spring of wet cases, as shown in Figures 23b and 23d. These confluent flows consist of the northwesterly associated with cyclonic circulation to the north of Korea and Japan and the south-westerly associated with anticyclonic circulation of the subtropical high. Thus, the WNPSH in dry cases is much weaker than that in wet cases from spring to summer. Such variation in the WNPSH in the spring may lead to the change in the summer monsoon rainfall over East Asia. As shown in Figures 23c and 23d, the height anomaly pattern in the summer of wet cases is opposite to that of the dry cases; the negative anomaly of the height at 850 hPa is located over the Korean peninsula and Japan in wet cases, whereas the positive anomaly is located in the same position in dry cases.

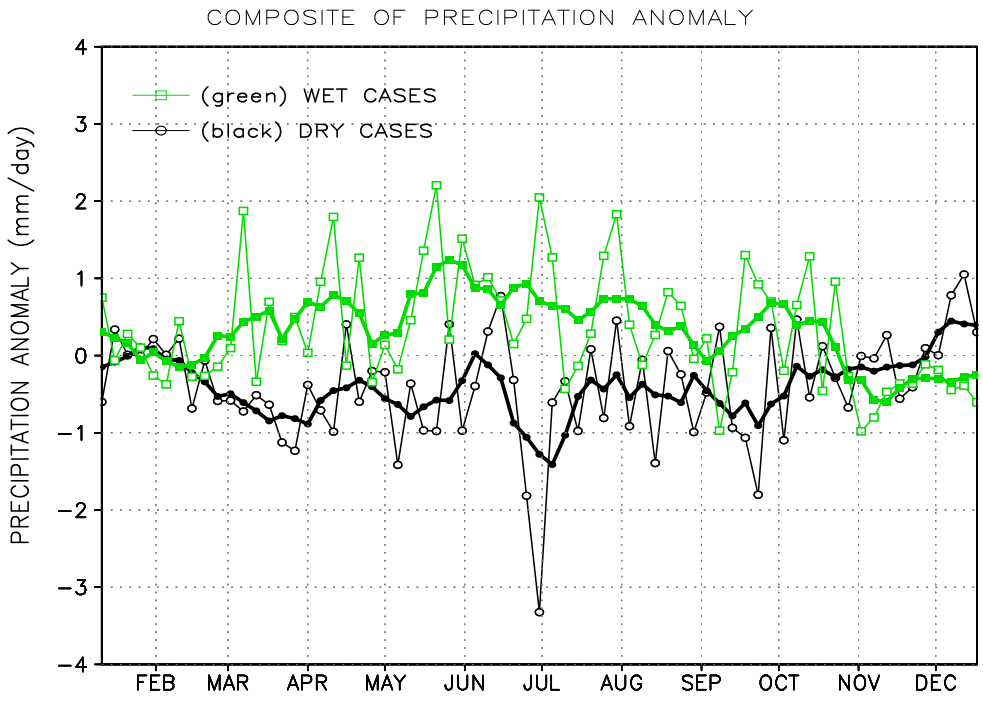

Figure 20. Composite of precipitation anomalies averaged over the region of 30°N–40°N, 110°E– 140°E for six dry cases (black curve) and six wet cases (green curve). The smoothed curves with dots denote three-pentad running means. The unit of precipitation anomalies is mm/day.

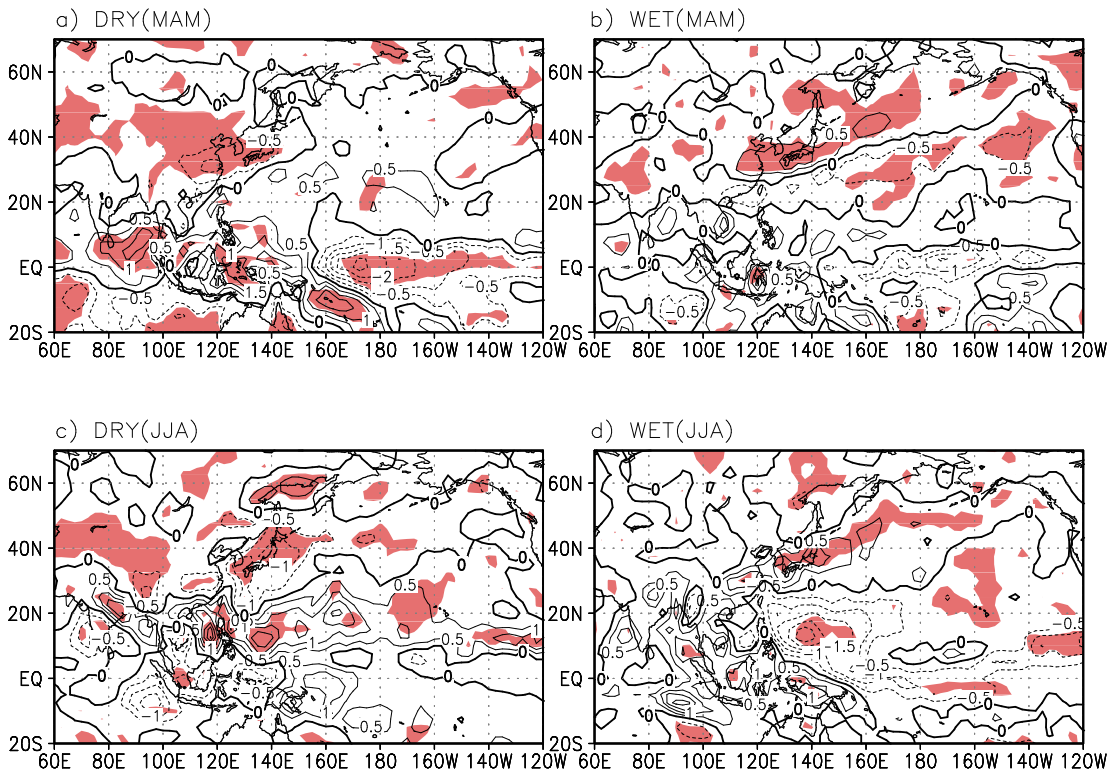

Figure 21. Composite anomalies of the precipitation for (a) the spring in dry cases, (b) the spring in wet cases, (c) the summer in dry cases, and (d) the summer in wet cases. The shaded areas indicate the statistical significance of the 95% confidence level. The unit of precipitation anomalies is mm/day

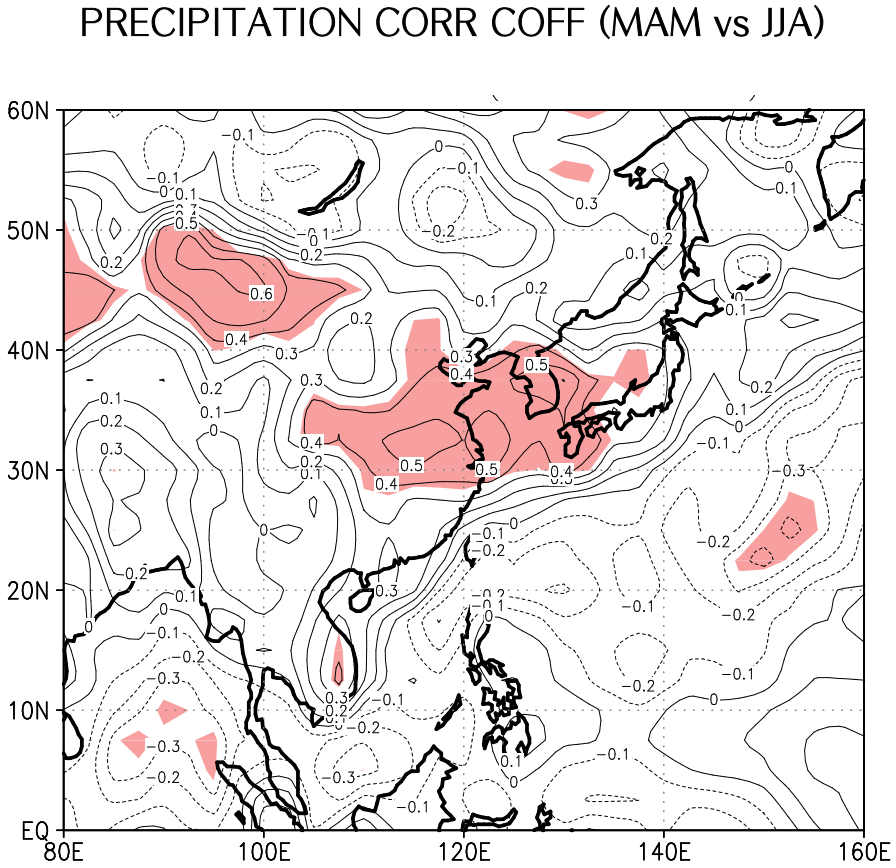

Figure 22. The correlation coefficients between time series of precipitation anomalies over the region 30°N–40°N, 110°E–140°E during spring and the precipitation field in the summer. The shaded areas indicate the statistical significance of the 95% confidence level.

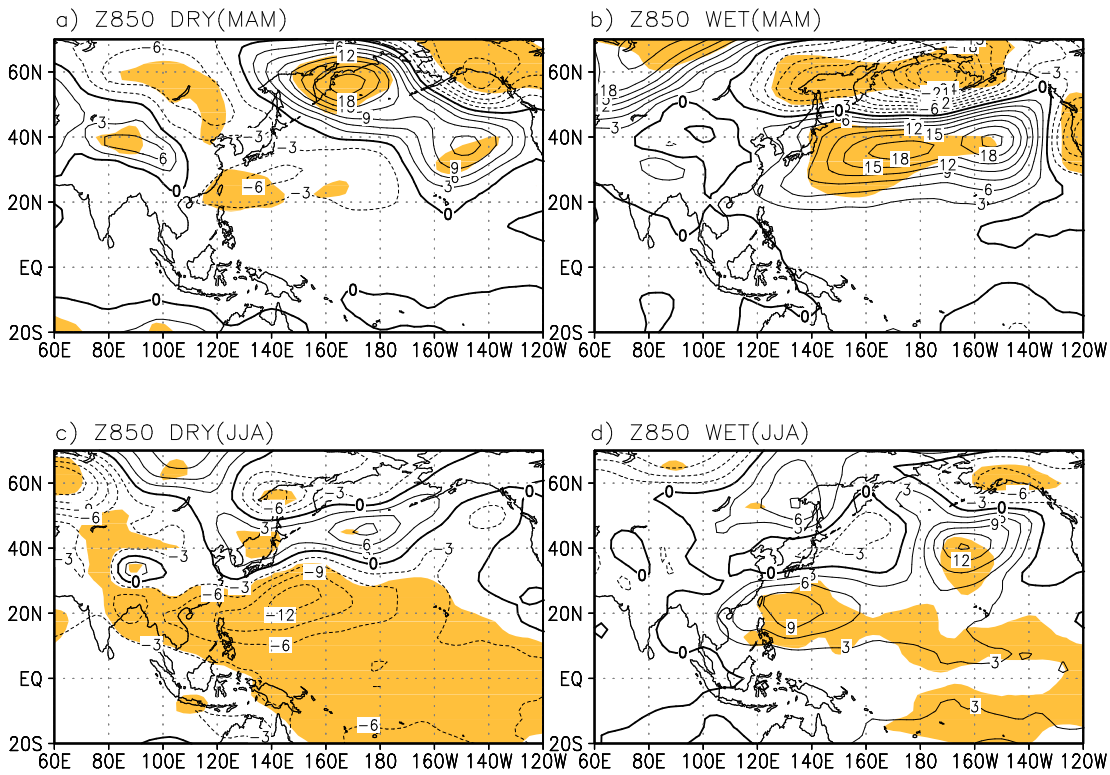

Figure 23. As in Figure 21 except for the geopotential height at 850 hPa. Units are gpm

The height anomaly pattern, with negative values over northeast Asia and positive values over WNP, in the summer of wet cases is associated with the intensification of the westerly (Lau and Li, 1984). There is little difference between the horizontal distribution and intensity of the height anomaly at 200 hPa and 850 hPa. In other words, the height anomaly pattern at 200 hPa is very similar to that at 850 hPa, except for the vertical structure with the northwestward tilt with height in wet cases (not shown) (Kang et al., 1999). The pressure system associated with the rainfall band in northeast Asia has a vertical structure with a northwestward tilt with height that is consistent with that of the vertical structure in the wet cases. The barotropic structure in the extratropical region may be disturbed by a thermally forced baroclinic response (Kurihara and Tsuyuki, 1987). This barotropic-baroclinic mode coupling could be an essential factor for the tilted vertical structure of the anomalies (Kosaka and Nakamura, 2006).

4.4. Zonal Wind Anomalies at 200 hPa

The EAWJ is closely linked to anomalies of large-scale circulation and East Asian spring and summer precipitation over northeast Asia. Previous studies have indicated that the north-south displacement of the upper level jet stream plays an important role in determining not only the onset and retreat of the monsoon but also the amount of monsoon rainfall (Yeh et al., 1959; Liang and Wang, 1998; Lau et al., 2000; Zhou and Wang, 2006). The zonal wind speed anomalies at 200 hPa are analyzed to identify both the variability of the westerly jet stream position and the relationship between the jet variation and rainfall anomalies (Figure 24). Positive and negative zonal wind speed anomaly patterns span the coastal region of East Asia and the western North Pacific in both dry and wet cases. In the spring and summer of the dry cases, zonal wind speeds increase over the WNP region and decrease over Korea and Japan, whereas in wet cases, these patterns are reversed. The variability of zonal wind speed in the spring is much larger than in the summer in both the dry and the wet cases.

The climatological mean position of the jet stream moves northward during the spring (Kuang and Zhang, 2005). This northward migration of the EAWJ is associated with the onset of the East Asian summer monsoon (Li et al., 2004). Because it is difficult to identify the jet stream shifts from the anomaly

distributions of zonal wind speeds, the mean positions of the jet axis in the dry and wet cases were investigated for the period from 1979 to 2007 (not shown). The jet locations in the dry case are shifted southward by 3° compared with the climatological mean position. For wet cases, these anomalous circulation patterns are somewhat different from dry cases. The EAWJ is displaced northward by 3° compared with the climatological mean position in the spring but southward by 2° in the summer. Although the anomalous circulation patterns are similar between spring and summer, the summer pattern is southward displaced noticeably in comparison to the spring pattern. In addition, the axis of climatological EAWJ locates further southward in the spring than in the summer.

On the basis of the thermal wind relation, the strong zonal wind speed normally appears in the frontal area of the troposphere. The temperature anomalies, which are averaged from 1000 hPa to 300 hPa, reveal that the strong positive anomaly is exhibited in the western North Pacific region and the strong negative anomaly in the region of southeastern China, Korean Peninsula, and Japan (Fig. 16). This north-south distribution of temperature anomalies is associated with the southward displacement of the EAWJ.

Lu (2004) proposed that the change in the location of the rainfall belt in East Asia is closely related to the meridional shift of the EAWJ. Therefore, when the location of the EAWJ moves southward and droughts may occur in the

Korean Peninsula and its surrounding regions. Also, the anomalous positive maximum zonal wind speed south of Japan in the spring of the dry cases indicates a southward shift in the climatological EAWJ pattern. The significant southward-shifted EAWJ in the spring and the summer of dry cases seems to be connected to the rainfall associated with the convection over the Philippines, as shown in Figures 10a and 10c. This feature is consistent with previous work showing that the convective activity over the Philippines is strongly associated with the EAWJ (Lu, 2004).

4.5. Moisture Flux Anomalies at 850 hPa

The moisture flux in the lower troposphere is one of the important factors giving rise to the suppression or increase of precipitation over a local area (Trenberth and Guillemot, 1996). Therefore, we have examined how the transport of moisture contributes to precipitation over East Asia and which moisture sources over the western Pacific, Indian Ocean, and South China Sea are important for the precipitation variability over northeast Asia.

In this study, the moisture flux is constructed using the wind vector anomalies and the specific humidity anomalies at 850 hPa in the springtime of the analysis period (29 years). Figure 25 shows the difference between the moisture fluxes in the spring of the dry and wet cases. The contours are the differences between precipitation anomalies in the two cases; the shadings are the negative anomalies. This composite difference, spring in the dry cases minus spring in the wet cases, represents changes in the moisture transport and convergence zone during the spring between the dry and wet cases. The moisture flux in Figure 25 identifies two moisture sources: the western Pacific and the Indian Ocean across from the Bay of Bengal. During the dry years, the northward moisture flux is dominant over the western Pacific (10°N–28°N, 100°E–140°E), but this northward flux is prevented by a strong westward

moisture flow in the region of 30°N– 35°N, 110°E–140°E. During the wet years, the source of moisture flux transported to the Korean Peninsula originates from the Indian Ocean. This pattern in dry cases is associated with the moisture divergence over the northeast Asian region.

Owing to the cyclonic circulation over the WNP, inflows from the Indian Ocean, Bay of Bengal, and the western flank of WNPSH are decreased in dry cases. Thus, the intensity variation of the WNPSH plays an important role in controlling the moisture supply from the tropics to the Korean Peninsula. The characteristics in the dry pre-monsoon season can be summarized as the lack of precipitation, which is well matched with the shaded area in Figure 25, and the weakened moisture inflow toward the Korean Peninsula, the heavy rainfall over the Philippine Sea, a weakened WNPSH, and a southward shifted EAWJ. These conditions persist to the summer monsoon season.

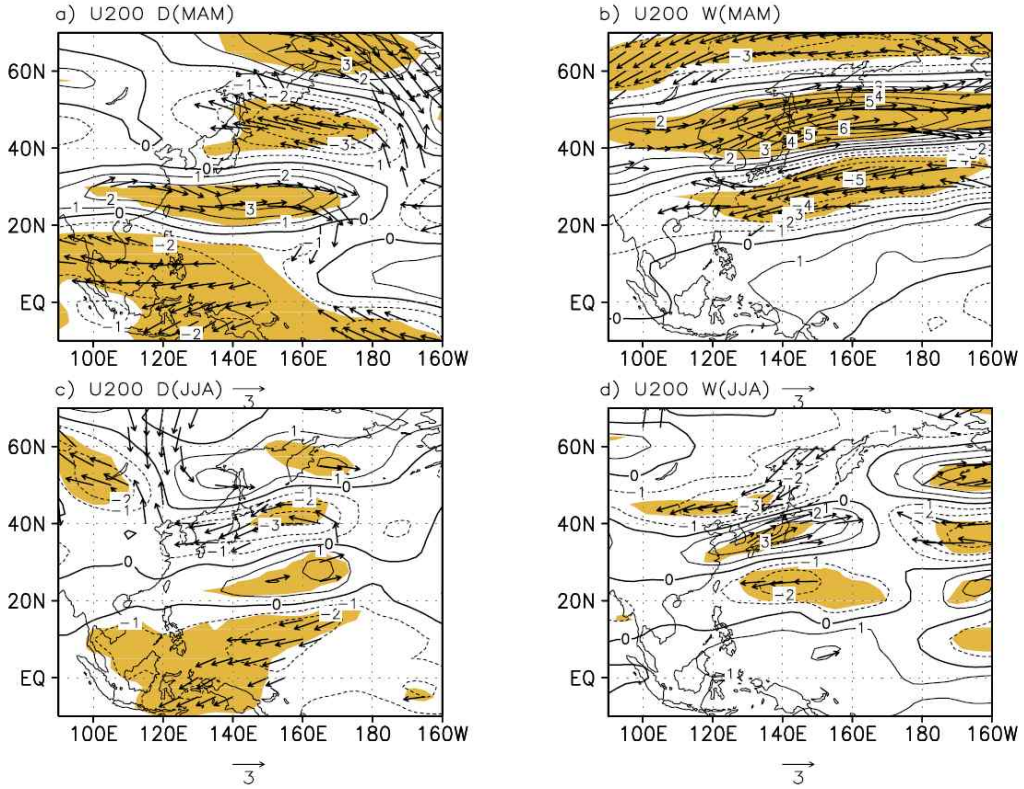

Figure 24. As in Figure 21 except for the zonal wind speed and wind vector at 200 hPa. Wind vectors only with the significance of 95% are denoted. Units are m/s.

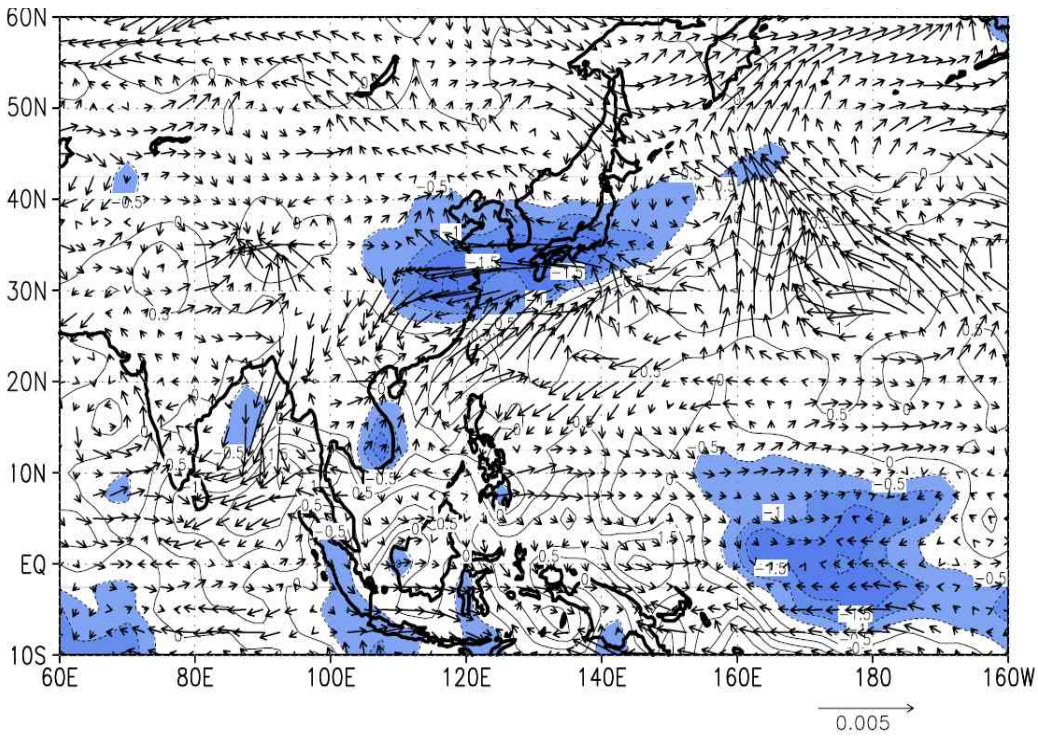

Figure 25. The moisture flux (arrow) and precipitation anomaly (contour) differences in spring between dry and wet cases. The unit of moisture flux is (g/kg) (m/s). Shadings indicate negative anomalies of precipitation difference. The contour interval is 0.5 mm/day.

4.6. Linkage of the anomalous circulations and SST anomalies

The abovementioned analysis reveals that the atmospheric circulation anomaly lasts from spring to summer. However, the atmosphere has a short memory: the anomaly itself cannot persist from spring to summer. The SSTs used as conditions last much longer than the variables, such as wind and pressure, which often provide a memory to the atmosphere (Namias, 1982).

Thus, to examine how the SST anomaly pattern in the tropical Pacific affects the large-scale circulation and thermodynamic moisture over East Asia, we present composites of the SST anomaly in Figure 26. These composites from winter to summer for the dry and the wet cases are analyzed. The seasonal variation of SST anomaly patterns for both the dry and the wet cases in Figure 26 shows the persistence from the previous winter to the summer. Because the SST forcing, in general, has a long memory, the anomalous circulation patterns over the northeast Asian region and the WNP region in the summer could be affected by SST anomaly forcing in the spring as well as in the summer.

A noticeable feature of the dry cases (Figures 26b, 26c, and 26e) is that the warm SST anomalies in the western Pacific are extended southwestward and continued from the winter to the summer. In general, the amplitude of warm SST anomalies (0.4°C ~0.3°C) in the western Pacific is significantly maintained to

summer, although this values are becoming weakened by 0.1 in JJA. On the basis of these results, we identified that the possible forcing in dry cases is related to the western Pacific (Figures 17a and 26c). The anomalous warm SST over the WNP leads to a strong convection over the Philippines and its surrounding areas (Figure 17a). Then, this anomalous convection causes positive precipitation anomaly in the Philippines owing to a strong ascending motion, whereas droughts occur in Korea and Japan owing to a descending motion through the local Hadley circulation. Simultaneously, these anomalous vertical motions may influence the meridional temperature gradient and thus change the jet stream, as shown in Figure 15a (Trenberth et al., 1988), as well as the seasonal march of the WNP subtropical high. The WNP subtropical high in dry cases is significantly weaker compared with that in wet cases (Figure 14); these negative anomalies become more enhanced in the summers of dry cases.

In wet cases, warm SST anomalies dominate over the Indian Ocean and they extend to the northeast Asian region. This SST anomaly pattern is associated with the moisture flux shown in Figure 25, which indicates that the external forcing in wet cases exists in the Indian Ocean, as shown in a previous study (Zhou and Wang, 2006). Zhou and Wang (2006) pointed out that summer precipitation anomalies over the South China Sea are associated with SST anomalies in the Indian Ocean and the South China Sea. They also demonstrated

that these summer precipitation anomalies are linked to the spring Hadley circulation. The above analysis indicates that the location of the external forcing in dry cases is clearly different from that in wet cases. The forcing in dry cases comes from the western Pacific and the forcing in wet cases comes from the Indian Ocean. The role of anomalous SST and anomalous convection in the western Pacific from winter to summer is probably to suppress moisture inflow from the south toward the East Asian region during the spring in dry cases. This condition continues until the summer monsoon season, which makes the spring and summer dry in northeast Asia.

As shown by previous subsection 3.4.3, Fig. 26 remarkably appears cold SST anomalies to the south of Korean peninsula and Japan, extratropical Pacific Ocean (25°N-35°N, 130°E-160°E), in both the dry case and wet case, although the anomalous cold SST anomalies in dry case is not much more significant than those in wet case. In particular, the intensity of cold SST anomalies in dry cases is growing lower by 0.2°C as season goes from DJF to JJA. Thus, the confidence level is decreased and do not also present persistence. Whereas, in wet cases, warm SST anomalies in that region rather become more strengthened than previous season and demonstrated persistent feature. However, some previous studies have shown that the effect of extratropical SST anomalies is less significant than that of tropical SST through the model simulation. According to

Yoo et al. (2004), the forcing by the extratropical Pacific SST anomalies in uncoupled model experiments show insignificant impact on the East and Southeast Asian climate. This reason for the model results is probably contributed to the lack of air-sea interaction. For this reason, the present study excludes effect of extratropical Pacific SST anomalies in model experiments expecting to deal with in next section.

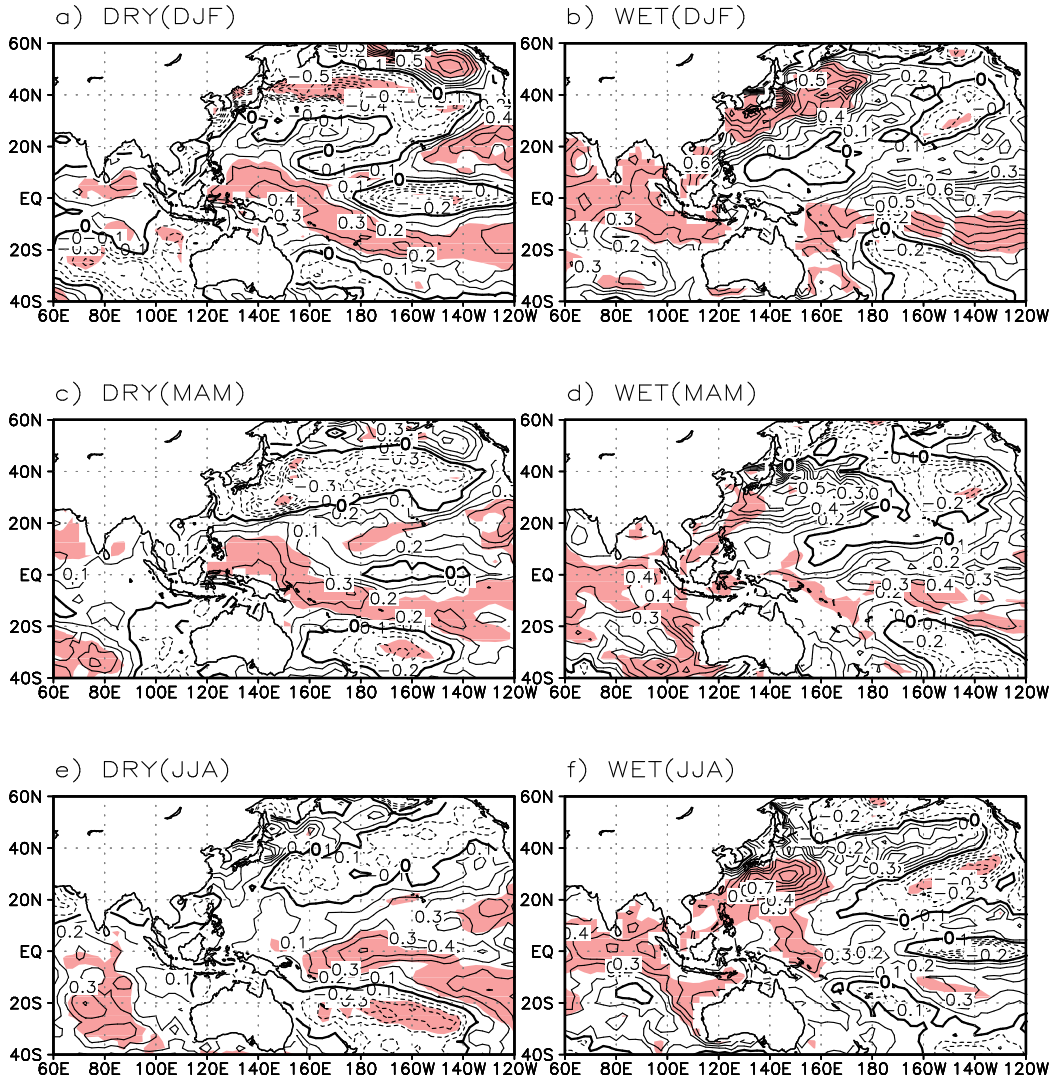

Figure 26. Composite anomalies of sea surface temperatures: (a) December to February (DJF) mean in dry years, (b) DJF mean in wet years, (c) March to May (MAM) mean in dry years, (d) MAM mean in wet years, (e) June to August (JJA) mean in dry years, and (f) JJA mean in wet years. The shaded areas indicate the statistical significance of the 95% confidence level. The contour interval is 0.10C.

5. Result of Model Experiments

5.1. Model and Experimental Design

In order to examine the response of atmospheric circulation on SST forcing of western Pacific and Indian Ocean, which is based on observational SST anomalies in dry and wet cases(Figure 27 and 28), model experiments have been performed. The model simulation is focused on the demonstration of the impact of western Pacific and Indian Ocean on dry case and wet case, respectively. We used the Seoul National University AGCM (SNUAGCM) global spectral model in our experiment. This model has been used in previous studies on the Asian monsoon and ENSO (Wang et al., 2004). It has a T31 horizontal resolution (approximately 2.5 latitude x 3.5 longitude). There are 17 unevenly spaced sigma-coordinated vertical levels in the model. A more detailed description of this model is given by J.-K. Kim et al. (East Asian summer monsoon simulated by the Seoul National University GCM, paper presented at International Conference on Monsoon and Hydrologic Cycle, Korean Meteorological Society, Kyungju, South Korea, 1998).

We have performed five experiments: the control, Dry Force western Pacific (WP), Wet Force WP, Dry Force Indian Ocean (IO), and Wet Force IO

runs. The main differences among these experiments are the imposed locations of the anomalous SST forcing. A list of the above mentioned experiments, along with a brief explanation, is presented in Table 1. Each of these experiments involves five ensemble members with varying initial conditions. Integration of seven months (from February to August) is performed for each simulation. The specified SST forcing is based on the observed SST data averaged for dry and wet cases. To investigate the consistency of the data with observational data obtained from the reanalysis products described in section 3, model outputs are compared with the composite analysis results of dry and wet cases in Figures 23 and 24. Note that the anomalies in all the model experiments are obtained by subtracting the control run results. The comparison is focused on the intensity and location of the WNPSH at 850 hPa and the north-south displacement of the EAWJ at 200 hPa.

5.2. Circulations at 850 hPa in Dry/Wet Force Run

Figure 29 shows the geopotential height anomaly fields at 850 hPa, which respond to the imposed SST forgings in the western Pacific and the Indian Ocean in the spring and summer of the dry cases. In case of the Dry Force WP experiments, the whole patterns of anomalous geopotential height are similar to the aforementioned observations (Figures 23a and 23c). The Dry Force WP experiment results show the whole patterns of anomalous geopotential height which are similar to observations, but the Dry Force IO experiment results show the totally different from observations. In the experiment results for the springtime, the negative anomaly exists over the Korean Peninsula and the strong positive anomaly over the Aleutian region like the observations in Figure 29a, whereas the positive and negative anomalies locate over the Korean Peninsula and the Aleutian region, respectively in Figure 29c. A weakened WNPSH in the summer can be seen in Figure 29b as in Figure 23c, while there is no significant anomaly over the WNP region in Figure 29d. In addition, the wave train pattern from the WNP is obvious in Figure 29b, while there is no significant wave train and there exists the strong positive anomaly over the southeastern China in Figure 29d. However, the amplitude of anomaly, especially in the spring, (Figure 29a) is much larger than observations, which seems to be due to a

bias of AGCM because of no air-sea interaction. Thus, the SST in the western pacific rather than the Indian Ocean could lead to anomalous circulation fields at 850 hPa over the northeast Asia and the WNP regions from spring to summer.

According to these, the results from the Dry Force WP run are much closer to the actual observations than those from the Dry Force IO run. The Dry Force WP and Dry Force IO simulations estimate the relative effect of the regional SST forcing on the weakening of the WNPSH during the dry years. In the case of Dry Force IO (MAM), the pattern is totally different from that of the Dry Force WP (MAM). This implies that the SST in the Indian Ocean does not lead to anomalous circulation fields of 850 hPa over northeast Asia and the WNP regions.

Contrary to the Dry Force WP experiment, the Wet Force WP (MAM) pattern of Figure 30a is not well simulated based on comparisons with actual observation anomalies. The signs of anomalies in the model simulation are opposite to those in the actual observations: negative over the Korean Peninsula and positive to the north (Figure 30a). On the other hand, when MAM SST anomalies are imposed over the Indian Ocean in the wet cases, the effect of Indian Ocean SST is revealed in the zonal band of 20°N–40°N. In the Wet Force IO (MAM) run, the signs of anomalies in the simulation are similar to observations, which are positive over the WNP region and negative to the north

(Figures 30c and 23b). However, the Wet Force IO (JJA) pattern is relatively well matched to the observations (Figures 30d and 23d). Therefore, the warm SST anomalies over the Indian Ocean from the spring to the summer of wet cases lead to the wet conditions over northeast Asia until the summertime.

5.3. EAWJ at 200 hPa in Dry/Wet Force Run

The simulated zonal wind speeds at 200 hPa in the Dry Force WP and Dry Force IO experiments are shown in Figure 31. This simulation shows the north-south displacement of the EAWJ location and the intensity of the EAWJ responding to SST forcing in the dry cases. The most striking result is that this simulation shows the southward movement of the EAWJ. The EAWJ in the Dry Force WP (MAM) run is well simulated in terms of the locations of positive and negative anomaly centers of zonal wind speed compared with the Dry Force IO (MAM) run (Figures 31a, 31c, and 24a). That is, the spring pattern resulting from the Dry Force IO run shows the EAWJ shifted southward compared with observations. In the summer pattern of the Dry Force WP run, the simulation gives better results than in the spring. However, in the Dry Force IO (JJA) experiment, the pattern of anomalies of the zonal wind speed is much different from the observations in terms of anomaly center (Figures 31d and 24c). Thus, the persistence of the response pattern from the spring to the summer is also similar to that of the aforementioned observations (Figures 31a, 31b, 24a, and 24c).

Figure 32 shows the simulated EAWJ for wet cases. The Wet Force IO run gives better results concerning the anomalous zonal wind speed pattern at 200 hPa than the Wet Force WP. In the outputs for the summer, the anomalous

pattern from the Indian Ocean SST forcing such as the strengthened upper zonal wind speed over Korea and Japan and the weakened one to the north of this region is similar to the observations (Figures 32d and 24d). However, the anomalous pattern from the western Pacific SST forcing has the distribution of anomalous zonal wind speed with opposite signs to the observations (Figures 32b and 24d). Although the meridional position of jet core from the Indian Ocean SST forcing in spring is not similar to the observations, on the whole, Indian Ocean SST forcing seems to contribute to the zonal wind speed at 200 hPa. Therefore, the warm SST over the WNP region seems to lead to the southward movement of EAWJ in the dry cases, whereas the warm SST over the Indian Ocean seems to lead to the displacement of EAWJ in the wet cases, especially in the summer.

Table 1. Explanation of the model experiments

Experiments	Locations of specified anomalies of SST Forcing
Control	None
Force WP	Tropical Western Pacific (20°S−20°N, 100°E−170°E)
Force IO	Indian Ocean (20°S−20°N, 30°E−100°E)

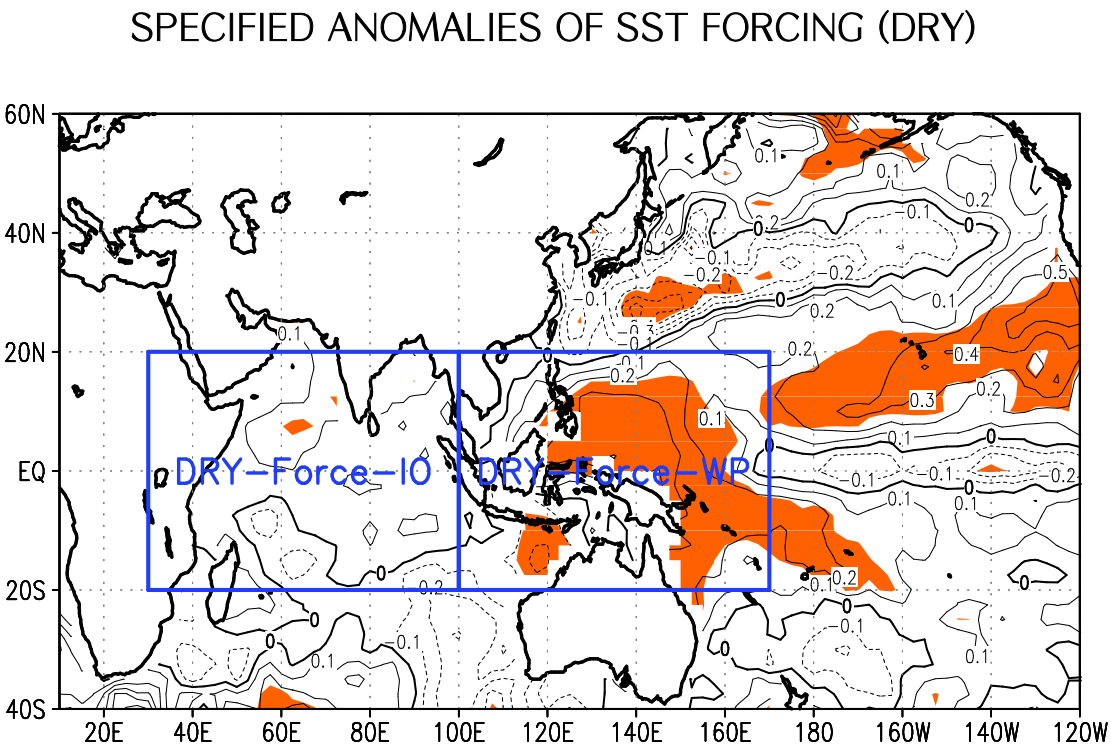

Figure 27. Specified anomalies for SST forcing in western North Pacific for dry case

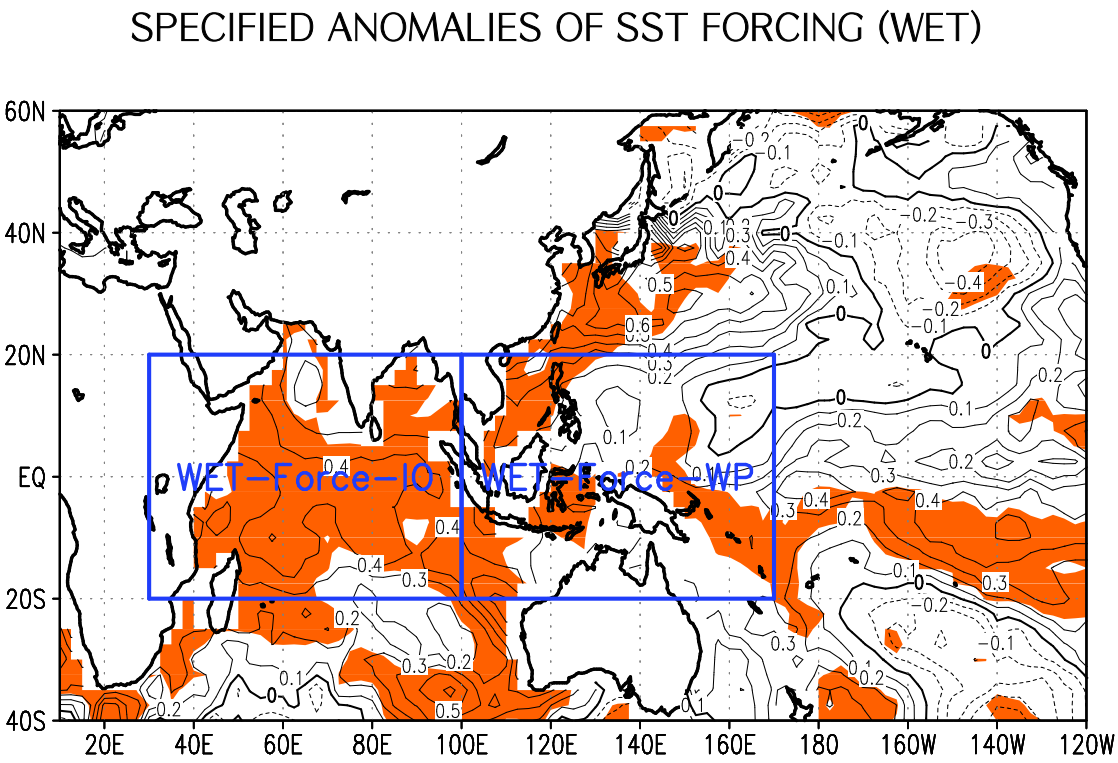

Figure 28. Specified anomalies for SST forcing in Indian Ocean for wet case

MODEL RESULT: DRY FORCING (850 hPa)

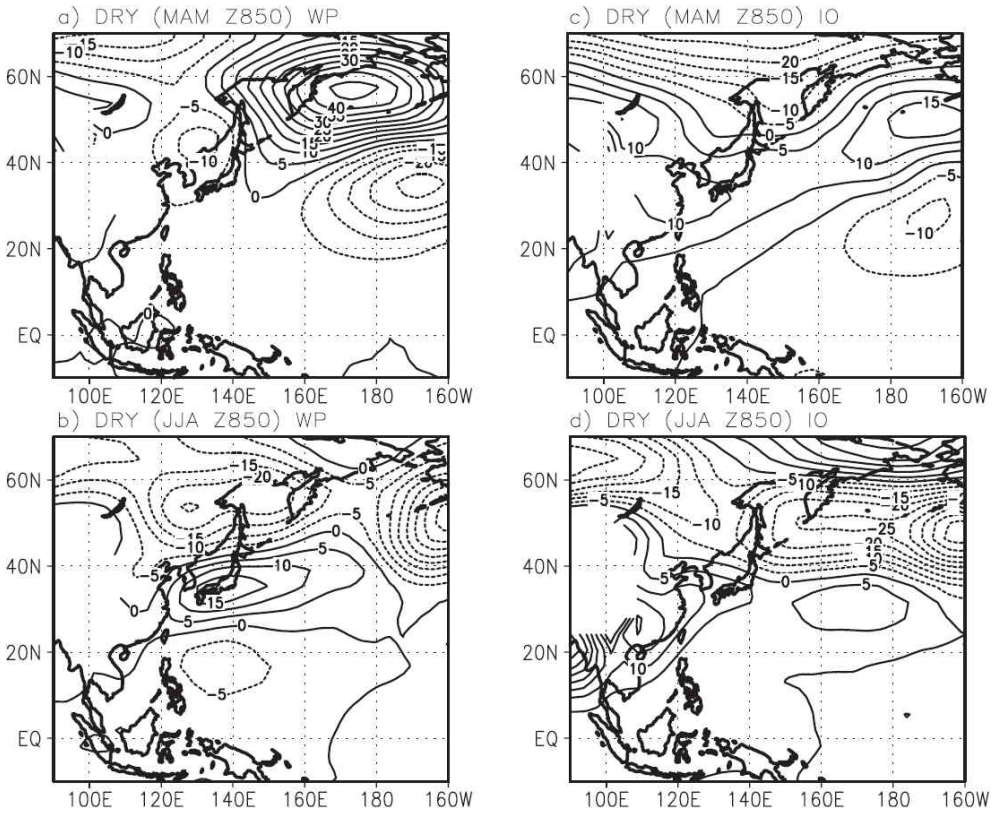

Figure 29. Model results of geopotential height anomalies at 850 hPa in dry years: (a) MAM Force WP experiment, (b) JJA Force WP experiment, (c) MAM Force IO experiment, and (d) JJA Force IO experiment.

MODEL RESULT: WET FORCING (850 hPa)

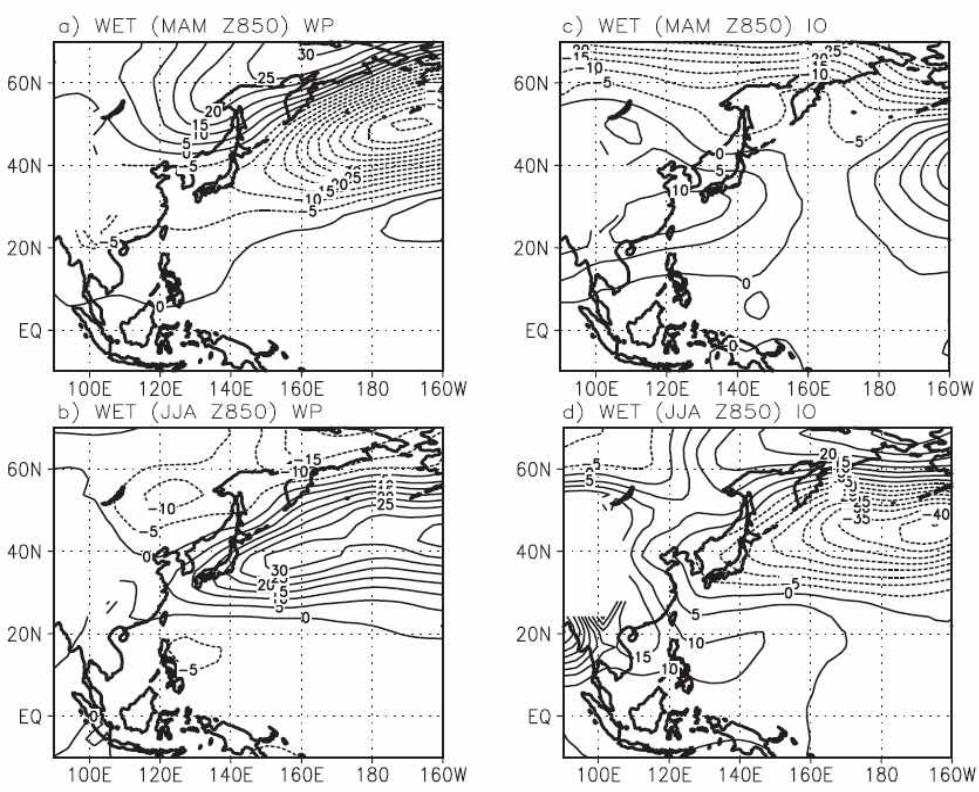

Figure 30. As in Figure 29 except for wet years.

MODEL RESULT: DRY FORCING (U200)

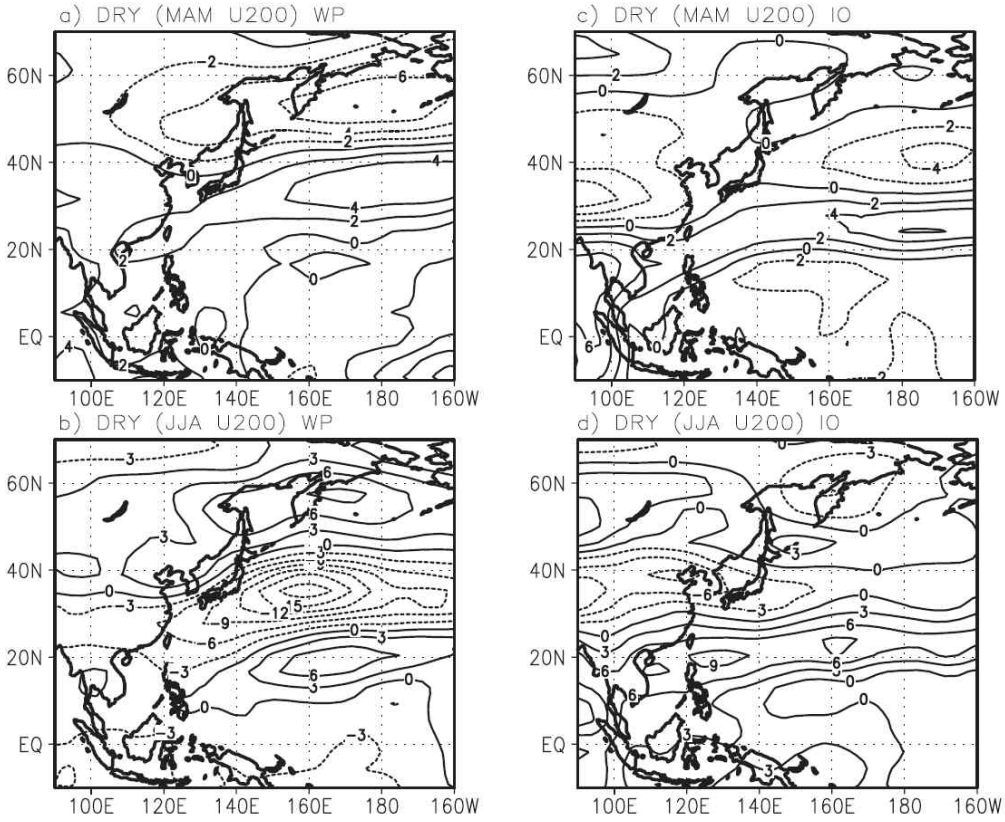

Figure 31. As in Figure 29 except for zonal wind speed anomalies at 200 hPa.

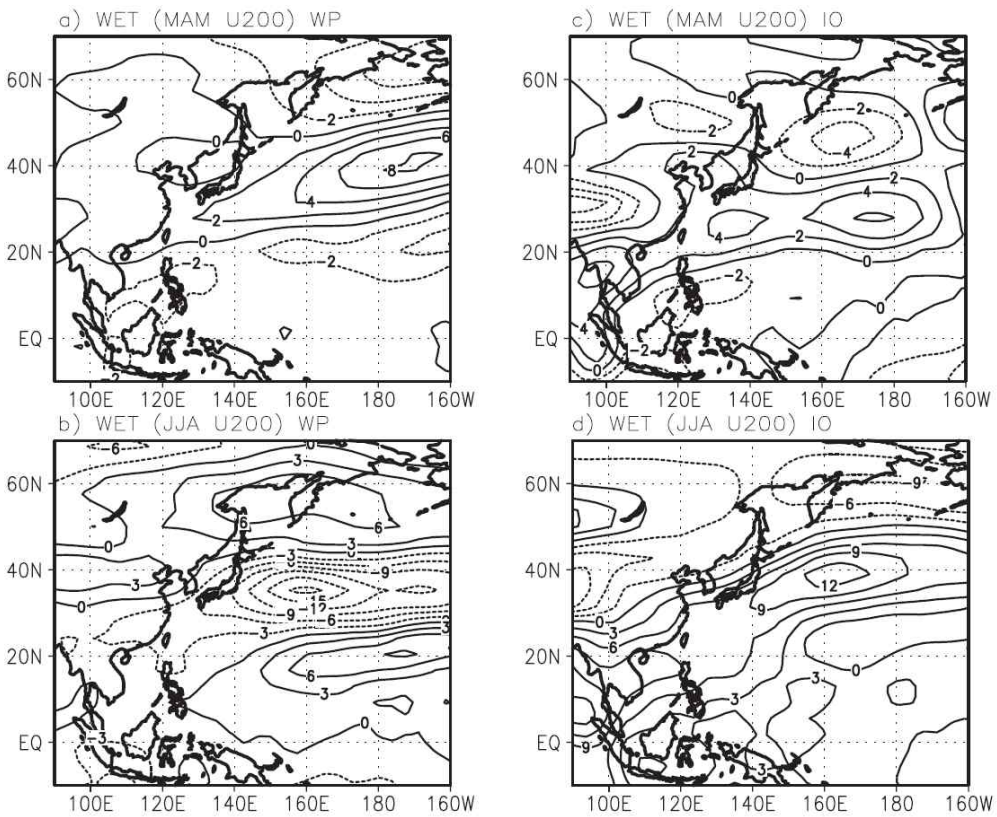

Figure 32. As in Figure 31 except for wet years.

6. Summaries and Conclusions

Characteristic of atmospheric circulation anomalies over northeast Asian region were analyzed from spring to subsequent summer and their persistence were also investigated on the dry and wet cases during same period. This present study was focused on the dry cases in the premonsoon season and described into two parts; one issue is about the specific features of spring drought over the Northeast Asian region, the other is about the persistence and the associated characteristic large-scale circulation anomalies of such a extreme precipitation like drought over the same region from spring to following summer.

The prominent features of anomalous circulations in spring droughts 1960 to 2005 have been analyzed using the PDSI produced as an indicator of the severity of droughts. We have obtained the meaningful prominent characteristics in the spring drought over northeast Asia. In the mean wind field at 850 hPa, dominant anticyclonic circulation to the south of northeast Asia and significant cyclonic circulation to the north of the same location can clearly be seen. On the other hand, the opposite can be seen in drought years; that is, cyclonic circulation to the south and anticyclonic circulation to the north. Cyclonic circulation in the Western Pacific indicates that the WNPSH becomes weakened and the

associated moisture flux transported northward along the flank of the WNPSH is significantly diminished. The jet stream core, at 200 hPa in drought years, is shifted further southward than that of the mean field by 3°–5° latitude. This new jet stream position is nearly consistent with the location of the rainfall band in the composite map during drought years. The significant northerly winds over the region of 18°N–32°N, 110°E–120°E probably lead to the weakening of the northward moisture transport from the lower latitude and thus the anomalous rainfall band is established 5° –10° further southward than the mean field.

It is important to note that the warm SST anomalies in the Western Pacific play an important role in modulating atmospheric circulation. The warm SST anomalies and the associated convection in the Western Pacific, as well as the cold SST anomalies to the north of the warm SST anomalies, can be termed the north–south dipole pattern. We have defined the EAWJ index in an effort to understand how SST anomalies cause changes in the location of the jet stream and the related precipitation variability. It was found that the change in the EAWJ location and the associated rainfall anomalies in spring drought years were significantly associated with the north–south dipole pattern. The north–south dipole pattern was indeed consistent with other atmospheric circulation anomalies. Therefore, we could infer that the anomalous Western Pacific convection and the associated moisture anomalies give rise to a latent

heat release, which, in turn, causes changes in vertical motions; that is, a descending motion over the North Pacific (Korea, Japan, and Southeast China: 30°N–40°N, 110°E–140°E) and an ascending motion in the Western Pacific due to Hadley circulation. These anomalous vertical motions lead to the southward displacement of the EAWJ because of the change in the horizontal distribution of temperature, the weakening of the WNPSH, and the absence of precipitation over northeast Asia. Additionally, the strong northerly wind (cyclonic circulation) due to weakening of WNPSH in the lower level over the region of 18°N–32°N, 110°E–120°E is another significant characteristic in spring drought years. Therefore, we suggest that the changes in the intensities of the WNPSH and the EAWJ seem to control the moisture transported into northeast Asia, while SST anomalies in the Western Pacific play an important role in adjusting the balance between the above two systems.

In the second place, to examine the persistence of extreme precipitation such as drought and the related circulation anomalies, large-scale circulation anomalies for dry and wet cases, defined from levels of spring precipitation over Northeast Asia, have been analyzed from 1979 to 2007. We have used the precipitation data to select and define the dry and the wet cases, since PDSI employed as reference of drought. The persistence of extreme precipitation from the premonsoon to monsoon seasons has been found. Through

composite analyses of some variables in the spring and the summer of dry and wet cases, the persistence of circulation has also been found. As noted in the previous section, for dry cases, the WNPSH is distinctly decreased and the EAWJ axis is displaced southward from the spring to the summer season. For wet cases, the WNPSH is strengthened and the EAWJ is displaced northward in the spring but southward in the summer. Interestingly, the circulation patterns in wet case have similarities in geopotential fields and wind fields. The results of dry cases are basically reversed to those of wet cases. However, SST anomaly patterns are asymmetric in both the dry and the wet years: dry cases are related to the western Pacific SST and wet cases are related to the Indian Ocean SST.

The patterns simulated using observational SST anomalies are well matched with observational composite results. The WNP SST is one of the most important factors in simulating lower level (850 hPa) and upper level (200 hPa) circulation anomalies from the premonsoon season to the summer monsoon season for the dry cases. In Dry Force WP run, negative anomalies of geopotential height at 850 hPa appear over the WNP region and the EAWJ axis at 200 hPa is shifted southward. On the other hand, Dry Force IO run reveals the opposite patterns of those actually observed.

In Wet Force IO run, the enhanced WNPSH is simulated through the effect of Indian Ocean's warming from spring to summer. While, in Wet Force

WP the SST anomaly in the WNP does not contribute to the enhanced WNPSH from spring to summer. In the simulation of EAWJ of the wet cases, the Indian Ocean SST acts as a positive effect in simulating the location of summer EAWJ in Wet Force IO run. The fact that the responses of the western Pacific and the Indian Ocean SSTs are nearly reversed in all simulated large-scale circulations is a very meaningful result. The WNP SST is important in leading to dry cases, and the Indian Ocean SST is essential for wet cases.

Through the observational analysis and model simulation, this study has shown persistence of extreme precipitation and the associated atmospheric circulation anomalies from premonsoon season to following monsoon season. These persistence atmospheric circulations are likely maintained by local atmosphere-ocean interaction through positive feedback.

Some possible mechanisms are proposed on the basis of previous description. When warm SST forcing is imposed in the western Pacific, the anomalous convection is enhanced over this region. These ascending motions due to SST forcing around 0°–20°N lead to the descending motions in the region of 30°N–40°N through the local Hadley circulation. The changes in the vertical motions affect the change in large-scale circulation, as well as the location and the intensity of the EAWJ. Through these atmospheric circulation anomalies and thermodynamic changes, the seasonal migration of WNPSH is changed (Wu and

Wang, 2000) and the precipitation over the northeast Asian region is suppressed. The linkage between atmospheric circulation anomalies and SST, a key system connecting extreme precipitation over the northeast Asian region and Philippine Sea surface warming, is the anomalous cyclonic circulation due to weakening of WNPSH over western North Pacific. These wind anomalies are produced and remained by a positive feedback resulting from thermodynamic coupling of the Rossby waves and SST warming over the WNP region. The notion is illustrated by systematic diagram in Fig. 33. From October to May, in cold season, mean winds are dominant by northeasterly trade wind over WNP region around Philippine Sea. As depicted in Fig. 33, to the east of an anomalous cyclonic circulation, the total wind speed and the associated evaporation and entrainment SST warming is maintained. This SST change, implying SST warming by induced wind anomalies over WNP, could be maintained through positive feedback by air-sea interaction.

A number of issues still remain. For example, previous studies have shown that the Indian Ocean plays an important role in producing summer monsoon rainfall (Lee et al., 2005) and in constructing the relationship between spring and summer rainfall anomalies (Zhou and Wang, 2006) over East Asia. Some studies on the 1994 summer drought over East Asia have been completed. One of reasons for this drought is the orographic influence over Tibet (Park and

Schubert, 1997) and another is an Indian Ocean Dipole effect (Guan and Yamagata, 2003). Therefore, for a more detailed mechanism of the persistent anomalous atmospheric circulation during extreme precipitation, we should investigate other effects, including an interaction effect between the Indian Ocean and the western Pacific SSTs in the premonsoon season and the EASM rainfall anomalies. In addition to the above results, it was found that the frequency of droughts in northeast Asia has been increasing since the 1990s, which may be related to variations in summer monsoon atmospheric circulation over East Asia since the mid-1990s (Kwon *et al*., 2005, 2007). A study of the relationship between spring droughts and summer monsoons in northeast Asia should be performed on the basis of long-term PDSI and precipitation data.

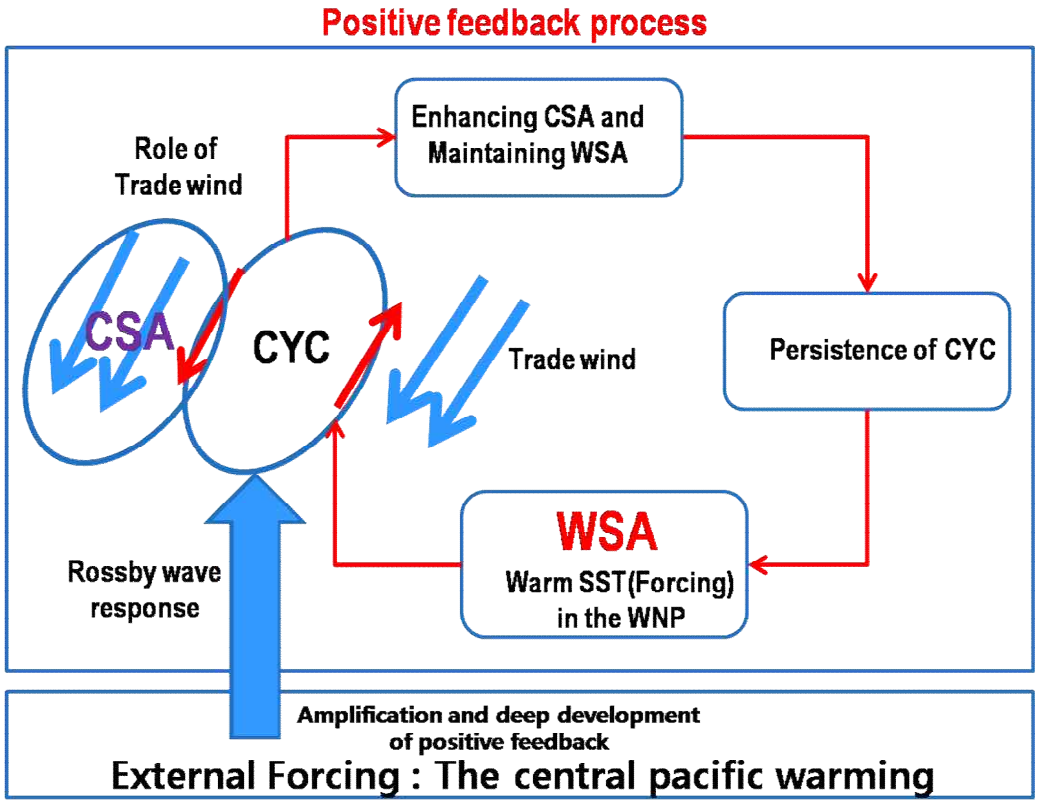

Figure 33. Schematic diagram of positive feedback processor between local wind and SST.

References

Alley, W. (1984), The Palmer drought severity index: Limitations and assumptions, *J. Climate and Appl. Meteor.,* **23**: 1100–1109.

Barlow, M., S. Nigam, and EH. Berbery (2001), ENSO, Pacific decadal variability, and U.S. summertime precipitation, drought, and stream flow. *J. Climate,* **14**: 2105–2128.

Byun, H.-R. (1991), A study on the existence of the dry period before the Changma and its associated atmospheric circulation, Ph.D. thesis, Seoul National Univ., Seoul.

Dai AI, Fung IY, Genio ADDel. 1997. Surface observed global land precipitation variations during 1900–1988. *J. Climate,* **10**: 2943–2962.

Dai, A. I., K. E. Trenberth, and T.R. Karl (1998), Global variations in drought and wet spells: 1900–1995. *Geophys. Res. Lett.,* **25**: 3368–3370.

Gong, D. Y., and C.-H. Ho (2003), Arctic oscillation signals in the east Asian summer monsoon, *J. Geophys. Res*., 108(D2), 4066, doi:10.1029/ 2002JD002193.

Guan, Z., and T. Yamagata (2003), The unusual summer of 1994 in east Asia: IOD teleconnections, *Geophys. Res. Lett*., 30(10), 1544, doi:10.1029/2002GL016831.

Hansen, J, and S. Lebedeff (1987), Global trends of measured surface air temperature. *J. Geophys. Res.,* **92**: 13345–13372.

Kalnay E, Kanamitsu M, Kistler R, Collins W, Deaven D, Gandin L, Iredell M,

Saha S, White G, Woollen J, Zhu Y, Chelliah M, Ebisuzaki W, Higgins W, Janowiak J, Mo KC, Ropelewski C, Leetmaa A, Reynolds R, Jenne R. 1996. The NCEP/NCAR 40-year reanalysis project. *Bull. Amer. Meteor. Soc.,* **77**: 437–471.

Kang, I.-S., C.-H. Ho, Y.-K. Lim, and K. M. Lau (1999), Principal modes of climatological seasonal and intraseasonal variations of the Asian summer monsoon, *Mon. Weather Rev*., 127, 322 – 340, doi:10.1175/15200493(1999)127<0322:PMOCSA>2.0.CO;2.

Kosaka, B. Y., and H. Nakamura (2006), Structure and dynamics of the summer Pacific-Japan (PJ) teleconnection pattern, *Q. J. R. Meteorol. Soc*., 132, 2009 –2030, doi:10.1256/qj.05.204.

Kuang, X., and Y. Zhang (2005), Seasonal variation of the east Asian subtropical westerly jet and its association with heating field over east Asia, *Adv. Atmos. Sci.*, 22, 831 –840, doi:10.1007/ BF02918683.

Kurihara, K., and T. Tsuyuki (1987), Development of the barotropic high around Japan and its association with Rossby wave-like propagation over North Pacific: Analysis of August 1984, *J. Meteo. Soc*. *Jpn*., 65, 237 –246.

Kwon, M., J. G. Jhun, and K. J. Ha (2007), Decadal change in East Asian summer monsoon circulation in the mid 1990. *Geophys. Res. Lett.,* **32**: L16709, DOI:10.1029.2007GRL023026.

Kwon, M., B. Wang, S. I. An, and J. S. Kug (2005), Decacal change in relation-ship between east Asian and WNP summer monsoon. *Geophys. Res.*

Lett., **32**: L16709, DOI:10.1029.2005GRL023026.

Lau, K. M., and M. C. Li (1984), The monsoon of east Asia and its global association, *Bull. Am. Meteor. Soc*., 65, 114 –125, doi:10.1175/1520-0477(1984)065<0114:TMOEAA>2.0.CO;2.

Lau, K. M., M. K. Kim, and S. Yang (2000), Dynamical and boundary forcing characteristics of regional components to the Asian summer monsoon, *J. Climate*., 13, 2461 – 2481, doi:10.1175/1520-0442 (2000)013< 2461:DABFCO>2.0.CO;2.

Lee, E.-J., J.-G. Jhun, and C.-K. Park (2005), Remote connection of the northeast Asian summer rainfall variation revealed by a newly defined monsoon index*, J. Climate*., 18, 4381 –4393, doi:10.1175/ JCLI3545.1.

Li, C., J. Wang, S. Lin, and H. Cho (2004), The relationship between Asian summer monsoon activity and northward jump of the upper westerly jet location (in Chinese), Chin. *J. Atmos. Sci*., 28, 641 –658.

Liang, X. Z., and W. C. Wang (1998), Association between China monsoon rainfall and tropospheric jets, *Q. J. R. Meteor. Soc.*, 124, 2597 –2623, doi:10.1002/qj.49712455204.

Lu, R. (2004), Associations among the components of the east Asian summer monsoon system in the meridional direction, *J. Meteor. Soc. Jpn.*, 82, 155 –165, doi:10.2151/jmsj.82.155.

Mo, K. C., J. R. Zimmerman, E. Kalnay, and M. Kanamitsu (1991), A GCM study of the 1988 United States drought. *Monthly Weather Review* **119**: 1512–1532.

Namias J. 1991. Spring and summer 1988 drought over the contiguous United States-Causes and prediction. *Journal of Climate* **4**: 54–65.

Namias, J. (1982), Some causes of United States drought, *J. Clim.*, 2, 1362–1380.

Palmer, W. C. (1965), Meteorological drought. *U.S. Weather Bureau Technical Paper* **45**: 58, [Available from NOAA/National Weather Service, 1325 East-West Highway, Silver Spring, MD 20910].

Palmer, T. N., and C. Brankovic (1989), The 1988 United States drought linked to anomalous sea surface temperature. *Nature* **338**: 54–57.

Park, C. K., and S. D. Schubert (1997), On the nature of the 1994 East Asian summer drought. *J. Climate* **10**: 1056–1070.

Park, C.-K., and S. D. Schubert (1997), On the nature of the 1994 east Asian summer drought, *J. Climatology*, 10, 1056 – 1070, doi:10.1175/1520-0442(1997)010<1056:OTNOTE>2.0.CO;2.

Rajagopalan, B, E. Cook, U. Lall, and B. K. Ray (2000), Spatiotemporal variability of ENSO and SST teleconnections to summer drought over the United States during the twentieth century. *J. Climate* **13**: 4244–4255.

Trenberth, K. E., and C. J. Guillemot (1996), Physical processes involved in the 1988 drought and 1993 floods in North America, *J. Climate*, 9, 1288 – 1298, doi:10.1175/1520-0442(1996)009<1288:PPIITD> 2.0.CO;2.

Trenberth, K. E., G. W. Branstator, and P. A. Arkin (1988), Origins of the 1988

North American drought, *Science*, 242, 1640 –1645, doi:10.1126/science.242.4886.1640.

Wang, B., and L. Ho (2002), Rainy seasons of the Asian-Pacific monsoon, *J. Climate*, 15, 386–398, doi:10.1175/1520-0442(2002)015<0386:RSOTAP> 2.0.CO;2.

Wang, B., and R. Wu (1997), Peculiar temporal structure of the South China Sea summer monsoon, *Adv. Atmos. Sci.*, 14, 177 –194, doi:10.1007/s00376-997-0018-9.

Wang, B., and X. Xu (1997), Northern Hemisphere summer monsoon singularities and climatological intraseasonal oscillation, *J. Climate*, 10, 1071 – 1085, doi:10.1175/1520-0442(1997)010<1071: NHSMSA>2.0.CO;2.

Wang, B., L. Ho, Y. Zhang, and M. M. Lu (2004), Definition of South China Sea monsoon onset and commencement of the east Asia summer monsoon, *J. Climate*, 17, 699 –709.

Weng, H. Y., K. M. Lau, and Y. K. Xue (1999), Multi-scale summer rainfall variability over China and its long-term link to global sea surface temperature variability, *J. Meteor. Soc. Jpn.,* 77, 845 –857.

Wu, R., and B. Wang (2000), Interannual variability of summer monsoon onset over the western North Pacific and the underlying process, *J. Climate*, 13, 2483 – 2501, oi:10.1175/1520-0442(2000)013<2483: IVOSMO> 2.0.CO;2.

Xie, P., and A. Arkin (1997), Global precipitation: A 17-year monthly analysis

based on gauge observations, satellite estimates, and numerical outputs, *Bull. Am. Meteor. Soc*., 78, 2539 –2558, doi:10.1175/1520-0477(1997)078<2539:GPAYMA>2.0.CO;2.

Yeh, D. Z., S. Y. Tao, and M. C. Li (1959), The abrupt change of circulation over the northern hemisphere during June and October, in The Atmosphere and the Sea in Motion, edited by B. Bolin, pp. 249 –267, Rockfeller Inst. Press, New York.

Yoo, S.-H., C.-H. Ho, S. Yang. H.-J. Choi, and J.-G. Jhun (2004), Influences of tropical Western and extratropical Pacific SST on East and Southeast Asian climate in the summer of 1993-94, *J. Climate*, 17, 2673 – 2687.

Zhou, B., and H. Wang (2006), Relationship between the boreal spring Hadley circulation and the summer precipitation in the Yangtze River valley, *J. Geophys. Res*., 111, D16109, doi:10.1029/2005JD007006.

Webb, R. S., C. E. Rosenzweig, and E. R. Levine (1993), Specifying land surface characteristics in general circulation model: Soil profile dataset and derived water-holding capabilities. *Global Biogeochemical Cycles* **7**: 97–108.

Wu, R., and B. Wang (2000), Interannual variability of summer monsoon onset over the western North Pacific and the underlying process. *J. Climate,* **13**: 2483–2501.

Xie, P., and A. Arkin (1997), Global precipitation: A 17-year monthly analysis based on gauge observations, satellite estimates, and numerical outputs. *Bull. Amer. Meteor. Soc.,* **78**: 2539–2558.

Xin, X., R. Yu, T. Zhou, and B. Wang (2006), Drought in late spring of South Chian in recent decades. *J. Climate,* **19**: 3197–3206.

국문초록

북동아시아 지역에서의 몬순기간 전 기간부터 몬순기간 동안 극한강수량과 관련되어 나타나는 대기순환 장 특성들이 분석되었다. 또한 이들 대기 순환 장의 특징적인 패턴과 강수량 간의 상관성 또한 분석되었다.

본 연구는 크게 두 부분으로 나누어 수행되었다. 하나는 본 연구는 몬순 전 건기 즉 봄철 (3 월~ 5 월) 가뭄에 중점을 두었기에, 먼저 봄철 가뭄에 특징적으로 나타나는 대기 순환장 패턴을 분석하고, 이런 특징을 발생시키는 가능 메커니즘을 제시하였다. 다른 하나는 가뭄 등 극한 강수량의 지속성을 알아보기 위하여, 분석기간을 몬순기간 (여름철)까지 연장하였고, 상대적으로 강수량이 많았던 때와 건조한 경우로 각각 나누어 4 가지 사례 (봄철 과우, 봄철 다우, 여름철 과우, 여름철 다우)에 대하여 분석하였다.

동아시아지역에서 발생하는 봄철 가뭄을 정의하는데 파머지수를 사용하였으며, 정의된 가뭄 해에서 북서태평양고기압이 현저히 약화 (저기압성 회전) 되었음을 알 수 있었다. 또한 동아시아 제트 축이 2° ~ 3° 정도 남하된 것을 알 수 있었는데, 이는 EAWJ (East Asian Westerly Jet) 지수 분석으로 확인되었다. 그리고 열대 서태평양 (10°S–20°N, 120°E–160°E) 주변 해수면온도의 상승이 뚜렷함을 알 수 있었다. 따라서 강수대가 남쪽으로 이동되었으며, 관련된 강수가 한국, 일본, 그리고 중국 남동지역에 억제되어

봄철 가뭄으로 나타난 것으로 보인다. 해수면온도 상승과 음의 지구장파복사량 어노말리가 북동아시아 지역과 필리핀 사이에서 남북 방향 이중패턴 (north-south dipole pattern)을 보이고 있는데, 이것은 해들리 순환으로 설명 가능하다. 봄 가뭄의 직접적인 원인은 앞에서 설명한 북서태평양고기압의 약화와 제트축의 남하이지만, 필리핀 부근 서태평양의 해수면온도의 상승이 근본적으로 중요한 역할을 한 것으로 생각된다.

두 번째 연구에서 북동아시아 지역에서 가뭄과 같은 극한 강수량이 몬순 전부터 몬순기간까지 지속성이 있다는 것이 발견되었다. 과우 해와 다우 해를 선정하는데 있어서 강수량 자료를 사용하였다. 이는 첫 번째 연구에서 사용한 파머지수는 가뭄에 중점을 두고 개발한 지수이기에, 포괄적으로 사용할 수 있는 강수량 자료를 사용하였다. 이번 연구에서는 관측자료에 기반을 두고 분석한 결과를 모델 실험을 통하여 확인하였다.

과우 해 (dry case)와 다우 해 (wet case) 모두 봄부터 여름까지 강수량과 이와 관련된 대기 순환장 특성이 지속되는 것을 볼 수 있었다. 봄 가뭄 분석에서 나타난 것과 마찬가지로, dry case 에서는 북서태평양 고기압의 약화와 동아시아 제트 축이 남하하는 경향이 뚜렷하였으며, wet case 에서는 dry case 와 반대 현상이 뚜렷함을 알 수 있었는데, 즉 북서태평양 고기압 강화되었고, 동아시아 제트 축은 북상하였다. 그러나 해수면 온도와의

관련성은 대기 순환장 특성과는 다른 패턴을 보였다. Dry case 의 경우는 열대 서태평양 해수면 온도의 상승이 봄 가뭄 과 같은 극한 강수량의 발생과 지속성을 유지하는데 좋은 조건을 만드는데 중요한 역할을 한 것으로 생각된다. 이와는 다르게, wet case 의 경우는 인도양과 뱅갈 만의 해수면 온도의 상승과 관련이 있는 것으로 분석되었다. 두 경우의 이러한 해수면온도 어노말리 특성을 모델 실험에 각각 반영하였다. 한번은 열대 서태평양에만 해수면온도 어노말리 강제력 (forcing)을 주고, 또 한번은 인도양과 뱅갈만에만 해수면온도 어노말리 강제력 (forcing)을 주어 모델 실험을 하였다. 수치실험 결과 관측에 기반을 둔 분석결과를 대체로 잘 모의 하였다.

본 연구에서는 관측자료에 기반을 둔 분석과 모델 실험결과를 바탕으로, 극한 강수량의 지속성과 관련된 메커니즘을 제시하고자 한다. 해수면온도와 가뭄과 같은 극한 강수량간의 연관성과 관련된 주요 시스템 (key system)은 북서태평양에 나타난 변이된 저기압성 회전, 북서태평양고기압의 약화로 발생된 어노말리, (anomalous cyclonic circulation)이다. 이러한 변이된 이상 바람 장은 북서태평양지역 (필리핀 해)의 해수면 온도 상승과 로스비 파 (Rossby wave)가 열역학적으로 커플링되어 나타난 양의 피드백과정에 의해서 생성되고 유지된다. 외부 강제력 (external forcing)이라 할 수 있는 동중 태평양의 해수면온도 하강은 또한 위에서

언급한 양의 피드백과정을 지속적으로 유지하고 강화시키는 데 중요한 역할을 하는 것으로 생각된다.

감사의 글

나의 박사과정을 보낸 시간들을 돌아 보면서 감사의 글을 쓸 수 있게 해주신 하나님께 감사와 무한한 영광을 돌립니다. 12 년 남짓의 박사과정은 나에게 있어서, 하나님께 더욱 가까이 나가게 해주시고, 인내와 기다릴 줄 아는 마음을 주신 값진 시간이었습니다. 그리고 하나님께서 여기까지 인도하심에 있어서 매 순간 하나님께서 동행하시고, 때로는 저에게 귀한 사람들을 붙여주셔서 도움 받게 하시고, 완성케 하신 은혜에 감사합니다.

박사과정을 들어올 수 있게 기회를 주시고, 직장생활과 병행을 하고, 늦은 나이에 공부하여, 때때로 힘들고 지치고 어려운 순간마다 저에게 다가오셔서 용기 잃지 않도록 격려해주시고, 그러면서도 학문적으로도 눈높이를 맞출 수 있도록 철저하게 지도해주셔서 오늘의 제가 있게 해주신 신 전종갑교수님께 머리 숙여 깊은 감사를 드립니다. 또한 저의 논문지도를 뒤늦게 기꺼이 맡아주시고, 늘 시간이 부족한 저를 배려해주셔서 무사히 학위를 마칠 수 있도록 학문적으로나 인간적인 도움을 아끼지 않으신 임규호 교수님께 더없이 감사 드립니다. 귀중한 시간을 할애하셔서 논문심사를 맡아주시고, 정확한 지적을 통해 연구방향의 맥을 잡아주셔서 결과가 더욱 빛나게 해주신 강인식 교수님과 제가 미처 생각지 못했던 부분까지 섬세하게 조언해주신 이동규 교수님, 결정하기 어려운 문제에 대해 해박한 연구경험을 바탕으로 명쾌한 결론으로 힘이 되어주신 한양대학교의 예상욱 교수님께 깊은 감사의 마음을 전합니다.

논문심사를 직접 해주시진 않았지만, 저의 학위 논문이 나오기까지 많은 관심과 인간적인 배려를 아끼지 않으시고, 논문 구성과 짜임새까지도 조언해 주신 김광렬 교수님에 대한 감사를 또한 잊을 수 없습니다. 대기과학이라는 학문을 깊이 알게 하시고, 최고의 가르침을 주신 박순웅 교수님, 윤순창

교수님, 허창회 교수님, 최우갑 교수님, 손병주 교수님께 감사 드립니다. 또한 가뭄연구에 대한 열정이 대단하시고, 저의 논문에 많은 관심을 보여주신 부경대학교 변희룡 교수님께도 감사를 드립니다.

지금은 뵐 수가 없지만, 학부와 석사과정을 지도해주셨고, 대기과학이라는 학문을 처음 알게 해주셨던, 살아계셨더라면 누구보다 기뻐하셨을 이화여대 이내영 교수님, 아직도 학문과 일에 대한 열정이 대단하셔서 얼마 전에 지질자원연구원장님으로 취임하신 김규한 교수님, 저의 크고 작은 일에 언제나 든든한 후원자 역할을 해주시는 유정문 교수님께 감사의 마음을 전합니다.

제 인생에 있어서, 잊을 수 없는 소중하고, 보람 있는 시간으로 기억되는 때는 회사를 잠시 휴직(2001. 12~2003. 2)하고 대기해양역학 실험실 후배들과 보낸 2 년여 기간이 아닌가 생각합니다. 나보다 대부분 열살 이상 차이 나는 어린 후배들이었지만, 배려심이 많았던 후배들의 도움이 있었기에 힘든 여정을 견딜 수 있었습니다. 이에 감사의 마음을 전합니다. 실험실의 본을 보여주고, 논문을 꼼꼼하게 검토해서 수정해주고, 같이 고민해주던, 기상연구관 이은정 박사, 지금은 전남대학 교수님이 된 철학적인 문병권 교수, 예보업무가 좋아서, 미래 총괄예보관을 꿈꾸는 이현수 사무관, 늦게 시작한 공부라 배워야 할 것도 많았던 제가 물어볼 때마다 내일처럼 친절히 가르쳐 주고, 너무 많은 도움을 주었던, 해양연구원 선임연구원 민호, 때로는 친구처럼 때로는 친동생처럼 어려운 고민거리를 같이 나누었던 암기력이 뛰어난 미국 하와이대학에 있는 소영이, 긴 공백기를 지나 박사학위 최종발표를 위해서 다시 시작한 최근까지도 소소한 일들 하나하나 도와준 우리 실험실에서 제일 착한 윤경이, 연구 분석결과에 대해 날카롭고 정확하게 지적해주던, 겉으로는 자유분방해 보이지만 학문적으로 철저했던

원무, 최종발표 때 미처 생각지 못했던 부분까지 챙겨주었던 승민이, 올 2 월에 화촉을 밝히는 실험실 막내 새림이 모두에게 너무 감사합니다. 같은 시기에 실험실에서 만나지는 못했지만, 기상청을 다니면서 어려운 문제를 함께 나누었던 차은정 연구관, 실험실에서는 선후배들과 격의 없는 대화를 즐겼지만, 지금은 한 아이 아빠로 깨가 쏟아지는 한철이, 언제나 소탈한 웃음으로 실험실을 밝게 만들어 주던 용문이, 지금 해양연구원에서 있는 원모, 독일에서 연구 중인 종연이, 그밖에 그 동안 실험실에서 만났던 여러 후배들 너무 감사합니다. 처음 논문을 시작할 때 테마를 잡는데, 도움을 주고, 분석한 결과를 확인 해준 극지연구소 김백민 박사의 고마움도 빠질 수 없고, 언제나 친절한 웃음으로 행정지원을 아끼지 않았던 류현희 조교에게도 감사의 마음을 전합니다.

기상청 근무를 하면서 학위과정을 병행할 수 있도록 여러 면에서 도움을 주신 고윤화 기상청장님을 비롯한 직원 여러분들께도 깊은 감사의 마음을 전합니다. 가뭄연구의 본을 보여주셨을 뿐 아니라, 저의 연구에 관심을 가져주시고, 지도를 아끼지 않으셨던 박정규 국장님, 늦게 시작한 학위과정의 어려움을 이해해 주시고 안부를 물어주시던 이희상 단장님 감사합니다. 오랜 기간 동안 지속했던 학위과정이었기에 일일이 다 열거 할 수는 없지만, 수없이 많은 업무의 공백을 이해해 주시고, 격려를 해주었던, 서애숙 대전청장님, 권태순 센터장님을 비롯한 국가기상위성센터 직원과 김진국 센터장님을 비롯한 기상레이더센터 직원 여러분께 머리 숙여 감사 드립니다. 특히, 주어진 환경을 잘 극복하면서 최선을 다해서 일하는 레이더분석과 함동주사무관, 박혜숙연구관, 김지현사무관, 김헌애주무관, 이양동주무관, 양희준주무관, 이호민주무관, 박향숙연구사, 백문희주무관, 이윤정주무관, 김희숙주무관, 전종혁주무관, 주세희주무관 모두들 정말 감사합니다. 학문과 지식탐구에 대한 열정이 아직도 식지 않은 이미자 선배님, 박사학위가

지연될 때 용기 잃지 않도록 격려해주던, 합리적이고 순발력이 뛰어난 손승희 과장, 늘 얼굴에 웃음이 떠나지 않고, 매사 긍정적인 김금란 과장, 언제나 일이 재미있다며 어려운 일도 마다하지 않는 이미선 과장에게 고마움을 전합니다. 항상 관심을 가져주고, 같이 있으면 에너지가 전달되는 전영신 과장, 또한 부경온 연구관, 백희정 연구관에게도 감사의 마음을 전합니다.

박사과정을 하면서, 어려운 일을 만날 때마다, 기도해주시고, 조언을 아끼지 않았던 동숭교회 담임 목사님을 비롯한 교인 여러분들께 감사의 마음을 전합니다. 항상 주일 예배마다, 명쾌한 설교로 하나님 말씀을 깨닫게 해주신 서정오 담임 목사님, 결정하기 힘든 일이 있을 때마다 같이 기도해주시고 위로해주시던, 최우영 목사님, 김성우 목사님, 최승필 목사님, 늘 인자하신 웃음으로 따뜻하게 다가와 주셨던 민성기 권사님, 주방 식당 봉사를 할 때 뛰어난 리더십으로 이끌어주셨던 카리스마가 넘치는 이종옥 권사님, 언제나 자상한 웃음으로 안부를 챙겨주시던 신문주 장로님 그밖에 저를 도와 주셨던 동숭교회 성도님들에게 깊은 감사를 드립니다.

평생을 자식들을 자랑스러워 하셨던 부모님의 은혜에 지면을 빌어 진심으로 감사 드립니다. 공직생활을 꼿꼿하게 하셨고, 그리 쉽지 않은 환경에서도 장남으로서 역할을 하시면서, 2 남 3 녀 우리들을 훌륭히 키워내서 오늘에 있게 한, 지금은 하늘 나라에 계신 아버지, 박씨 집안 맏며느리로서, 온갖 집안 대소사를 그 작은 몸집으로 치르시면서도, 자식들 뒷바라지에 소홀함이 없었던, 여든이 훌쩍 넘은 나이에도 총명함이 묻어나는 이 세상에서 제일 아름다운 우리 어머니 사랑하고 감사합니다. 미생물학계 학자로서, 학생들을 가르치는 교수로서 존경 받는 우리 집 기둥이자, 어머니, 아버지의 자존심이었던 오빠, 어려운 종손 며느리로서 수고하고 책임을

다하는 올케언니, 한국의 슈바이처라고 해도 과언이 아니며, 뛰어난 의술로 여러 질병으로 고통 받는 환자들을 따뜻하게 치료해주시는 이름난 명의 큰 형부, 서양화를 전공해서 예술가다운 면모도 있지만, 넉넉하고 착한 마음씨로 까칠한 동생인 나를 언제나 너그럽게 포용하고 받아주는 큰언니, 매사 신중하시고 때로는 고지식해 보여도 누구보다 따뜻한 마음을 가진, 대학에서 학생들을 지도하시는 유전공학 박사 작은 형부, 유순하면서도 우리 집 딸 중 제일 상냥한, 작은 형부와 함께 연구교수로서 아직도 왕성한 생화학분야 연구활동을 하는 작은 언니, 우리 집 막내여서 생각도 어릴 줄 알았는데, 어느 날 보니 우리 중 제일 합리적이고, 포용력 있는 마음을 가진 것을 보고 대견하게 여겼던, 반도체 기술 분야 박사가 되어 관련 분야에서 신기술 개발에 힘쓰는 유일한 남동생, 겉 모습은 약해 보여도 안으로 강하고, 매사에 철저하여 두 아이를 잘 키워준, 여자 직업 중 최고라는 고등학교 교사 작은 올케, 모두에게 진심으로 감사의 마음을 전합니다. 그밖에, 언제나 대견하고 서로 우애가 돈독한 조카들에 대한 고마움도 잊을 수 없습니다. 미국 유학 중인 찬엽이, 대학생 찬용이, 건축가를 꿈꾸는 찬우, 올해 대학에서 디자인을 전공하게 되었다고 기뻐하는 찬은이, 길거리 캐스팅 될 정도의 외모는 물론 실력 또한 출중한 잘생긴 영호, 엄마의 재능을 이어받아 그 누구보다 최고의 작품전을 왕성히 열고 있는 서양화가 영은이 에게도 감사합니다.

직장생활을 하면서, 또한 박사과정까지 힘들게 병행하는 저를 항상 믿어주시고 지지해주셨던 시부모님께 진심으로 감사의 마음을 전합니다. 어려운 가운데서도, 자식들만은 고생시키지 않겠다는 일념으로 고단하게 사신 보람으로 한 가정을 일으켜 세우시고, 스킨 스쿠버 다이빙도 거뜬하게 하시는 건강한 체력과, 교회에서는 신앙생활도 모범적으로 하셔서 노년이 넉넉하고 멋진 아버님, 자식들에 대한 헌신적인 사랑과 강한 생활력을 갖고

계셔서 많은 생활 노하우를 저에게 전수해주셨고, 직장 생활로 며느리 노릇이 부족했던 저를 많이 참아주시고 배려해주신 시어머님께 이 자리를 빌어 감사의 마음을 드립니다. 자상한 성격으로 때때로 시동생이 아니라 시누이로 착각할 만큼 말없이 도와주고 챙겨주는 교수님 시동생, 피아노가 전공인 작은 동서, 시댁에서 일어나는 크고 작은 일의 해결사이면서, 분위기 메이커로서, 본인보다는 다른 사람을 배려하는 마음이 따뜻한 하나밖에 없는 시누이, 자상하고 상냥하여 같이 모여서 이야기를 해도 재미있는 소문난 내과 의사 선생님인 시누이 남편, 사업가로서 발전해 나가는 세 아들 중 가장 효자인 막내 시동생, 힘든 상황에서도 타인을 배려하는 막내 동서에게 감사한 마음을 전합니다.

그리고 이제 이세상에서 가장 소중하고 사랑하는 우리 가족 이야기를 할까 합니다. 박사과정을 처음 들어 갈 때부터 오랜 박사기간 내내 언제나 한결같이 묵묵히 물심 양면으로 지원해주고, 철저하고, 명석한 두뇌로 학교 공부는 물론 집안 일까지도 외조를 아끼지 않았던 동갑 나기 남편의 지지와 도움이 없었다면 포기했을지도 모르는 순간 순간들이 있었기에, 사랑하는 남편에게 이 자리를 빌어 진심으로 감사의 마음을 전합니다. 일하면서, 공부하는 엄마를 자랑스러워 했던 우리 사랑하는 두 아들에게도 감사의 마음을 전합니다. 겉으로는 강해 보여도 속으로 한없이 정이 많고 따뜻하고, 타인을 배려할 줄 아는 아빠의 명석한 머리를 닮아 머리 회전만큼이나 행동도 빠른 큰 아들 병연이, 눈웃음이 일품이고 한번 만나서 이야기하면 누구나 따르고 좋아하는 감성지수가 높은 장래희망이 대학 교수라는 작은 아들 기연, 우리 가족 모두 너무 사랑하고 고맙고, 자랑스럽습니다.

이제 끝으로, 다시 한번 하나님 아버지께 감사 드리고, 이 모든 영광을 하나님께 돌리며, 소중한 박사학위 논문을 하나님께 드립니다.